The Impact of Superior Mediastinal Lymph Node Metastases on Prognosis in Non-small Cell Lung Cancer Located in the Right Middle Lobe

Yukinori Sakao, MD, PhD, Sakae Okumura, MD,* Mun Mingyon, MD, PhD,* Hirofumi Uehara, MD, PhD,* Yuichi Ishikawa, MD, PhD,† and Ken Nakagawa, MD**

Background: We aimed to assess hilar and mediastinal lymph node involvement and its impact on prognosis in patients with right middle lobe lung cancer.

Methods: The records of 170 patients undergoing surgery for right middle lobe non-small cell lung cancer from 1980 to December 2007 were retrospectively examined. There were 45 patients found to have hilar or mediastinal lymph nodes metastases. This subgroup included 31 N2 patients and 14 N1 patients, and included 23 women and 22 men, whose ages ranged from 32 to 83 years (median = 61 years). The status of mediastinal, hilar, and interlobar lymph nodes was assessed according to the seventh edition of the TNM classification for lung cancer. Patient records were examined for age, gender, preoperative nodal status, surgical procedure, metastatic status of lymph nodes (distribution and numbers), tumor size, and histologic features (cell type and differentiation degree). Survival duration was defined as the interval between surgery and death from the tumor or the most recent follow-up.

Results: For N1 cases (n = 14), the most frequent metastatic site was #12m (lymph nodes adjacent to the middle lobe bronchus), which occurred in 11 cases; there was one case with metastases in #11s (lymph nodes between the upper lobe bronchus and bronchus intermedius), and no case with #11i metastases (lymph nodes between the right middle and lower lobe bronchi). The most frequent metastatic mediastinal zone was the subcarinal zone (25/31), and the superior mediastinal zone also had a high incidence of metastases (22/31). Sixteen cases had metastases to both the superior and subcarinal zones, and six cases had metastasis to superior mediastinal zone without subcarinal zone metastasis. When #11s or #11i was involved, eight of nine or five of five, respectively, were N2 cases. Univariate analyses revealed that tumor diameter, cN, status of lymph node metastases, and operative procedure (pneumonectomy) were significant prognostic factors in N2 cases. Regarding status of lymph node metastases, superior mediastinal zone metastases, both superior and inferior (subcarinal) zone metastases, and #11i were significant prognostic factors. Because #11i metastases and superior mediastinal lymph nodes metastases were highly correlated with each other (p = 0.02), two separate models were used in multivariate analyses. Superior mediastinal metastases (p = 0.03) and #11i metastases (p = 0.015) were revealed to be significant independent prognostic factors, whereas multiple-zone metastases only tended toward significance as an adverse prognostic factor (p = 0.054).

Conclusions: Superior mediastinal lymph node metastases and #11i metastases were significant adverse prognostic factors in patients with middle lobe lung cancer, and they were associated with each other.

Key Words: Middle lobe cancer, Superior mediastinal lymph node metastasis, N2, NSCLC.

(*J Thorac Oncol.* 2011;6: 494–499)

The right middle lobe is the smallest lobe in the lung, and lung cancer originating there is much less common than in the other lobes, occurring in 3.8 to 6.7% of all lung cancers.[1–4] The fact that it is less common may be a reason that there are a few reports on the prognostic factors of middle lobe lung cancer.

Lymph drainage from the middle lobe extends to both superior and inferior mediastinal lymph nodes, and previous reports have demonstrated a high incidence of metastases to both the superior and inferior mediastinal zones.[1–6] Nevertheless, there are few articles on the relationships between status of hilar and mediastinal lymph node metastases and patient prognoses.

In this retrospective study, we aimed to clarify prognostic factors in patients with middle lobe lung cancer who underwent surgery. Furthermore, we wanted to determine the association between the status of lymph node metastases and postoperative prognosis.

PATIENTS AND METHODS

This was a retrospective study. Because individual patients were not identified, our institutional review board waived the requirement for obtaining patient consent and approved this study. Between 1980 and December 2007, 170 patients underwent surgical resection at the Cancer Institute

Departments of *Thoracic Surgical Oncology and †Pathology, Japanese Foundation for Cancer Research, Cancer Institute Hospital, Tokyo, Japan.

Disclosure: The authors declare no conflicts of interest.

Address for correspondence: Yukinori Sakao, MD, PhD, Department of Thoracic Surgical Oncology, Japanese Foundation for Cancer Research, Cancer Institute Hospital, 3-10-6, Ariake, Koto-ku, Tokyo 135-8550, Japan. E-mail: yukinori.sakao@jfcr.or.jp

ISSN: 1556-0864/11/0603-0494

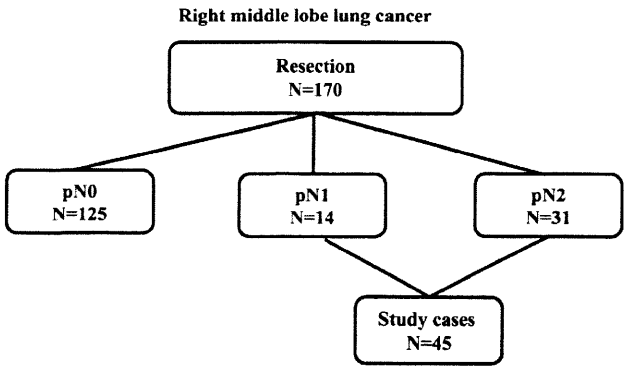

FIGURE 1. Study group subdivisions. Between 1980 and December 2007, 170 patients underwent surgical resections for right middle lobe lung cancer at the Cancer Institute Hospital. There were 14 N1 cases and 31 N2 cases evaluated.

Hospital for primary lung cancer originating in the right middle lobe. Among these patients, 45 were diagnosed with N1 or N2 disease after lung resection and hilar and mediastinal node dissections (Figure 1). The extent of lymph node dissection was not affected by a suspicion of N1 disease. We have routinely performed nearly the same dissection (ND2a).

All the 45 study patients were confirmed for their prognoses. The primary surgical procedure for lymph node dissection, such as hilar and mediastinal nodal dissection, was established in Japan in the late 1970s. In our institute, the extent of lymph node dissection conducted recently is nearly the same as that during the 1980s. Some cases had sampling due to disorders such as cardiac or pulmonary, and these cases were excluded from this study. The resected lymph nodes were separated according to the map[7] in the operating room by the surgeons. Station 10 nodes dissected in middle lobe cancer were adjacent to the inferior parts of the main bronchus, and these nodes were included in the subcarinal zone according to the new TNM. [7] The other station 10 nodes, which were adjacent to the upper parts of the main bronchus, were not routinely dissected, and this area is difficult to dissect without an upper lobectomy.

This subgroup included 31 N2 patients and 14 N1 patients, and included 23 women and 22 men, whose ages ranged from 32 to 83 years (median = 61 years, Table 1). For all patients, preoperative staging was performed using chest computed tomography (CT), abdominal CT or ultrasonography, brain CT or magnetic resonance imaging, and bone scans. Clinical mediastinal and hilar lymph node status was assessed as positive if the chest CT showed that the short axis of a node was more than 1.0 cm. CT scans have been used for evaluating lung cancer staging in our institute since 1980. Of course, CT imaging quality is different when comparing that in the 1980s with that in the 2000s. Nevertheless, this study focused on pathological N status of middle lobe lung cancer, and the quality of pathological examinations was nearly the same during the study period. We excluded those patients who had induction therapy because it seemed to be difficult to evaluate their pathological node status.

TABLE 1. Patient Characteristics

Age (yr)	32–83, median: 61
Gender (male/female)	22/23
c-N	
N0/N1/N2	23/14/8
c-T	
T1/T2/T3/T4	17/24/3/1
p-N	
N1/N2	14/31
Histologic type	
Adenocarcinoma/others	35/10
Well-differentiated/others	10/35
Surgical procedure	
Lobectomy/bilobectomy/pneumonectomy	21/14/10

Bulky N2 (shortest mediastinal lymph node diameter >2 cm) patients have not been candidates for surgery in our institute. Although mediastinoscopy, 18F-fluorodeoxyglucose positron emission tomography, or endobronchial ultrasound with transbronchial needle aspiration was applied to some patients in this series, they were not used for preoperative staging. Follow-up periods ranged from 2 to 302 months (median follow-up for living patients was 86 months).

The status of mediastinal, hilar, or interlobar nodes was assessed according to the seventh edition of the TNM classification for lung cancer.[7] Mediastinal nodes were classified into the following three zones: superior, subcarinal, and inferior. N1 nodes were classified into two zones as hilar or interlobar, and peripheral. The interlobar zone was divided into three subgroups as follows: #12m, lymph nodes adjacent to the middle lobe bronchus; #11s, lymph nodes between the upper lobe bronchus and bronchus intermedius; and #11i, lymph nodes between the right middle and lower lobe bronchi. When a case had mediastinal nodal involvement of two or more zones, it was classified with multiple-zone metastases.

Patient characteristics are summarized in Table 1. Patient records were examined for age, gender, preoperative nodal status, surgical procedure, metastatic status of lymph nodes (distribution and numbers), tumor size, and histologic features (cell type and degree of differentiation).

Statistical Analysis

Survival duration was defined as the interval between surgery and death from the tumor, or the most recent follow-up. Survival rates were calculated using the Kaplan-Meier method. Univariate analyses were performed using the log-rank test, χ^2 test, and logistic regression. Multivariate analyses were performed for variables with p values less than 0.1 by univariate analysis, using the logistic regression test in StatView J 5.0 (SAS Institute Inc., Cary, NC). A p value less than 0.05 was considered significant.

RESULTS

Status of Lymph Node Metastases

In N1 cases (n = 14), the most frequent metastatic site was #12m, occurring in 11 cases, and there was one case with metastases in #11s and 0 cases with #11i metastases (Figure 2).

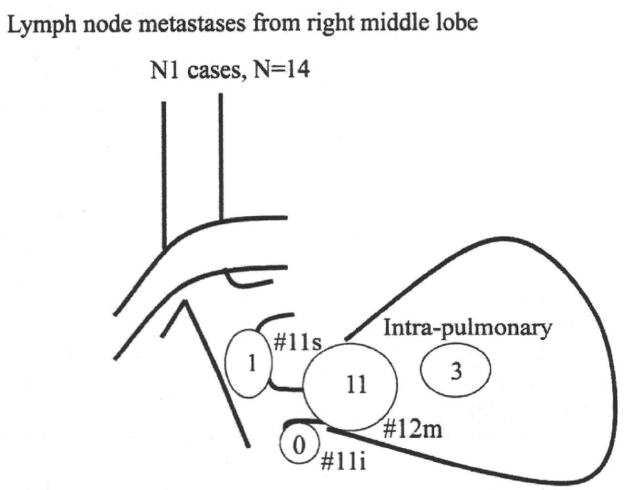

FIGURE 2. Distribution of metastatic nodes in N1 cases.

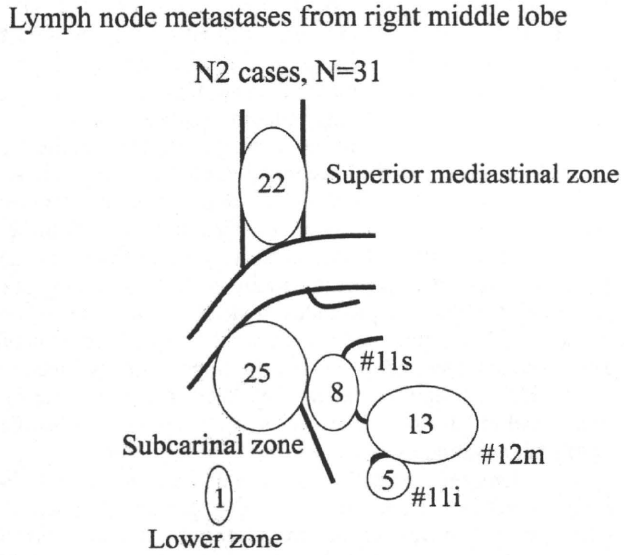

FIGURE 3. Distribution of metastatic nodes in N2 cases.

The most frequent metastatic mediastinal zone was the subcarinal zone (25/31 N2 cases). The superior zone also had a high incidence of metastases (22/31 cases). There were 16 cases with metastases in both the superior and subcarinal zones; nine cases were metastasized to the subcarinal zone without the superior mediastinal zone metastasis, and six cases were metastasized to superior the mediastinal zone without the subcarinal zone metastasis (Figure 3). When #11s was involved, eight of nine cases were N2, and when #11i was involved, all five cases were N2 (Figures 4 and 5).

Survival Rates for Patients with Nodal Involvement

The postoperative 5-year survival rate for patients with N1 was 62% and with N2 was 20% ($p = 0.02$). The postoperative 5-year survival rate was 83% for 125 N0 patients. The prognoses for N0 patients with right middle lobe cancers were not different from those of N0 patients with other involved lobes.

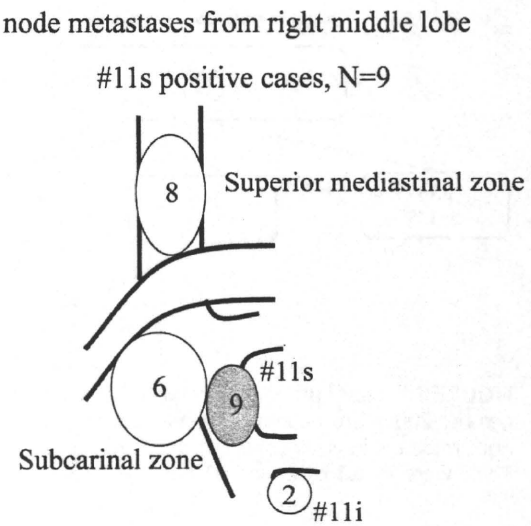

FIGURE 4. Association of #11s metastases with mediastinal zone metastases.

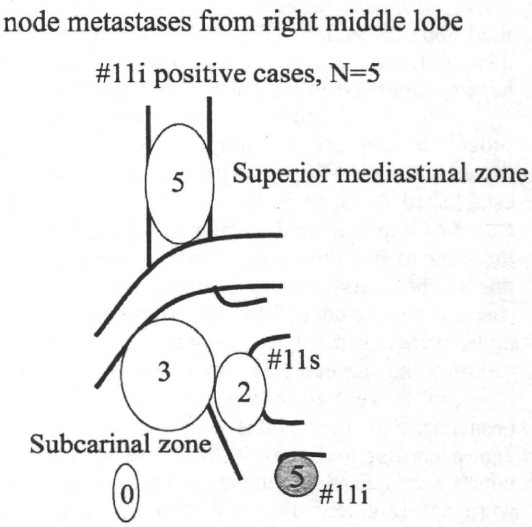

FIGURE 5. Association of #11i metastases with mediastinal zone metastases.

Prognostic Factors for N2 in the Right Middle Lobe

Univariate analyses using the variables listed in Table 2 showed that diameter, cN1–2/cN0, status of lymph node metastases, and operative procedure (pneumonectomy) were significant prognostic factors. Nevertheless, there was no difference in prognoses between lobectomy and bilobectomy. Regarding specific prognostic lymph node metastases, superior mediastinal zone metastases, both superior and subcarinal and interlobar #11i metastases were significant prognostic factors. Inferior mediastinal zone metastases, and #12m and

TABLE 2. Prognostic Factors for Patients with N2: Univariate Analysis

Variables	Cases	5-yr Survival (%)	*p*
Gender			
Male/female	14/17	17.8/22.0	0.95
Age			
<70 yr/70 yr or older	22/9	21.7/16.0	0.37
Diameter (14–65 mm, mean: 35 mm)			
<35 mm/35 mm or larger	16/15	36.5/6.8	0.02
cN			
cN1–2/cN0	15/16	8.0/33.7	0.042
cN0–1/cN2	23/8	23.3/12.5	0.24
Adenocarcinoma/others	26/5	25.2/0	0.1
Well differentiated/others	6/25	16.7/21.5	0.81
Pleural involvement yes/no	15/16	21.8/17.3	0.57
Status of lymph node metastases			
Superior mediastinal zone yes/no	22/9	6.4/50.8	0.005
Inferior mediastinal zone yes/no	25/6	21.4/16.7	0.61
#12m yes/no	13/18	24.7/18.3	0.92
#11s yes/no	8/23	14.3/21.9	0.14
#11i yes/no	5/26	0/23.6	0.02
Both superior and inferior zones			
Multiple zones/single zone	16/15	0/36.4	0.01
Operative procedure			
Pneumonectomy vs. others	7/24	0/25.8	0.009
Lobectomy vs. bilobectomy	16/8	23.6/29.2	0.61
Period			
Before 1995 vs. from and after 1995	15/16	13.3/28.4	0.28

#12m, lymph nodes adjacent to middle lobe bronchus; #11s, lymph nodes between the upper lobe bronchus and bronchus intermedius; #11i, lymph nodes between the right middle and lower lobe bronchi.

TABLE 3. Prognostic Factors for Patients with N2: Multivariate Analysis

Variables	Odds Ratio	95% CI	*p*
Model 1			
Diameter	1.04	0.99–1.08	0.054
cN			
cN1–2/cN0	1.87	0.71–4.95	0.21
Status of lymph node metastases			
Superior mediastinal zone	5.08	1.20–21.8	0.03
Multiple zones	1.42	0.51–3.96	0.50
Operative procedure			
Pneumonectomy	1.13	0.30–4.34	0.88
Model 2			
Diameter	1.03	0.99–1.06	0.17
cN			
cN1–2/cN0	1.38	0.54–3.52	0.51
Status of lymph node metastases			
#11i	4.80	1.34–17.0	0.015
Multiple zones	2.80	0.98–7.96	0.054
Operative procedure			
Pneumonectomy	2.32	0.62–10.0	0.20

#11i, lymph nodes between the right middle and lower lobe bronchi.

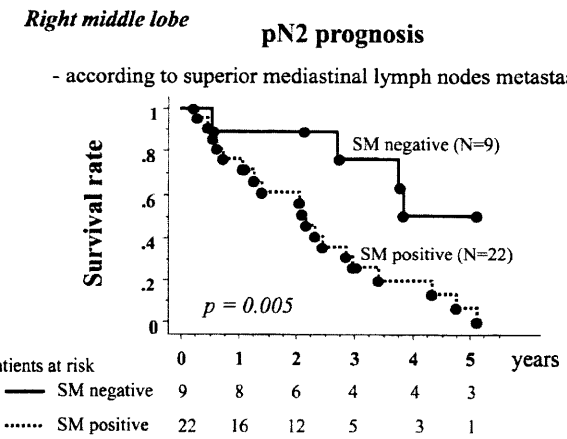

FIGURE 6. Postoperative survival according to superior mediastinal nodal involvement.

#11s metastases were not significant. There was no difference in prognoses between the patients before 1995 and patients from 1996 and after (5-year survivals of 13.3% and 28.4%; $p = 0.28$).

Significant variables by univariate analyses were analyzed by multivariate analyses (Table 3, models 1 and 2). Because #11i metastases and superior mediastinal lymph nodes metastases were highly correlated with each other ($p = 0.02$), two separate models were used for multivariate analyses. In model 1, superior mediastinal metastases were revealed to be a significant independent prognostic factor ($p = 0.03$). In model 2, #11i metastases were revealed to be a significant independent prognostic factor ($p = 0.015$), whereas multiple zone metastases only tended toward significance as an adverse prognostic factor ($p = 0.054$).

Survival Rate According to Prognostic N2 Factors

N2 patients were categorized according to whether they had significant prognostic factors determined from multivariate analyses, including superior mediastinal lymph nodes metastases, #11i metastases, or multiple mediastinal metastatic zones.

The 5-year survival rate was 50.8% in patients without superior mediastinal lymph nodes metastases, whereas it was 6.4% in patients with superior mediastinal lymph node metastases ($p = 0.005$, Figure 6). The 5-year survival rate was 23.6% in patients without #11i lymph node metastases, whereas there were no long-term survivors (dead within 3 years) in patients with #11i lymph node metastases ($p = 0.008$, Figure 7). Furthermore, the 3-year and 5-year survival rates were 58.2% and 36.4% in patients with single-zone mediastinal lymph node metastases, whereas they were 29.6% and 0% in patients with multiple-zone mediastinal lymph node metastases ($p = 0.01$), respectively. Nevertheless, by multivariate analysis, superior mediastinal lymph

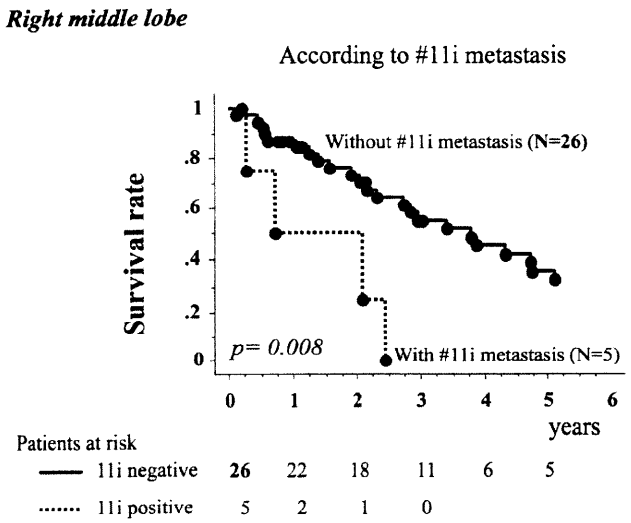

FIGURE 7. Postoperative survival according to #11i nodal involvement.

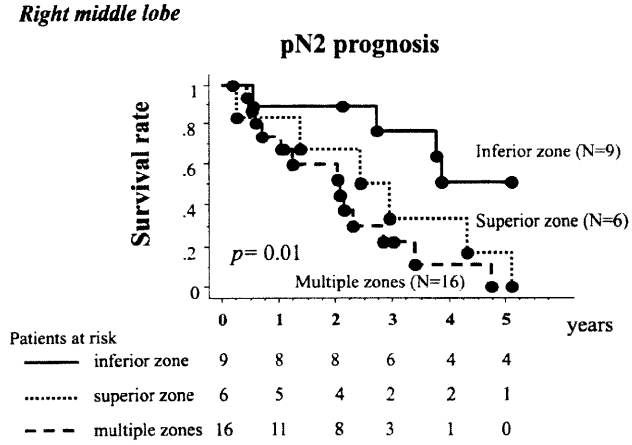

FIGURE 8. Postoperative survival: comparison of superior mediastinal nodal involvement with multiple-zone metastases.

node metastases were revealed to be a stronger prognostic factor than multiple metastatic zones (Figure 8).

DISCUSSION

There have been many reports on the prognostic impact of metastasis to specific mediastinal zones, especially lung cancer in the upper or lower lobes. For patients with lung cancer with tumor originating in the upper lobe or division, the frequency of subcarinal lymph node metastases has been reported to range from 3 to 5%, with the 5-year survival rates ranging from 9 to 18%.[8–10] The frequency of superior mediastinal lymph node metastases has been reported to range from 4 to 5%, with 5-year survival rates ranging from 0 to 19%.[10,11] This low-frequency mediastinal lymph node involvement was highly associated with multilevel N2, and therefore, the outcomes were poor.[10,12,13] In this study, the frequency of metastases was similar for the subcarinal and superior mediastinal zones, and the incidences in N2 patients were 80.6% and 71.0%, respectively. Thus, both superior and inferior mediastinal zones were found to be major metastatic sites, and these results are compatible with previous reports.[14]

We have revealed that metastases to the superior mediastinal lymph nodes are an important independent prognostic factor in patients with N2 middle lobe cancer. This is similar to what is seen in lower lobe cancer. Nevertheless, the incidence of skip metastasis to the superior mediastinum is very different between cancer in the middle lobe and in the lower lobe. The incidence in this study was 20% for N2 and has been reported to range from 3 to 4.5% in N2 right lower lobe cancer.[10–12] Furthermore, there was a significant difference in the 5-year survival rates for superior mediastinal involvement and inferior mediastinal involvement (6.5% and 50.8%, respectively), even for single-zone N2. When superior mediastinal lymph nodes were involved, the prognosis was almost the same as for multilevel N2 patients with middle lobe cancer.

The most frequent metastatic hilar lymph node was #12m, and most #11s and #11i metastases were found in N2 patients. In other words, metastases found in #11s or #11i indicate N2 disease (#11s: 8/9 and #11i: 5/5). Surprisingly, interlobar (lower lobe: #11i) lymph node involvement was an important adverse prognostic factor, even in N2 patients. This may be explained by the fact that there was an association between #11i metastases and superior mediastinal nodal involvement. Metastasis in #11i may be understood to be a result of mediastinal nodal involvement. That is, #11i metastasis is retrograde because of disturbed antegrade lymph drainage to the superior mediastinum from mediastinal metastases. Unfortunately, we could not find any previous reports regarding this correlation between #11i and superior mediastinal node involvement. Further investigation is needed to prove the hypothesis that #11i metastases result from superior mediastinal lymph node metastases.

In conclusion, superior mediastinal lymph node metastases and #11i metastases were significant adverse prognostic factors in patients with middle lobe lung cancer, and they were associated with each other. Furthermore, in patients with middle lobe lung cancer, #11i metastases may result from mediastinal metastases, and the impact on prognosis must be different from that of patients with cancer in other lobes.

Limitations of this study include its retrospective nature, including cases from the 1980s, a small sample number, and that routine adjuvant chemotherapy for N2 patients was started in 2006. Therefore, in this study, it was difficult to evaluate the effects on prognosis with respect to adjuvant chemotherapy.

REFERENCES

1. Vincent RG, Takita H, Lane WW, et al. Surgical therapy of lung cancer. *J Thorac Cardiovasc Surg* 1976;71:581–591.
2. Freise G, Gabler A, Liebig S. Bronchial carcinoma and long-term survival. Retrospective study of 433 patients who underwent resection. *Thorax* 1978;33:228–234.

3. Gifford JH, Waddington JKB. Review of 464 cases of carcinoma of lung treated by resection. *Br Med* 1957;30:723–730.
4. Ochsner A, Ray CJ, Acreea PW. Cancer of lung; review of experiences with 1457 cases of bronchogenic carcinoma. *Am Rev Tuberc* 1954;70:763–783.
5. Riquet M, Dupont P, Hidden G, et al. Lymphatic drainage of the middle lobe of the adult lung. *Surg Radio Anat* 1990;12:231–233.
6. Hata E, Hayakawa K, Miyamoto H, et al. Rationale for extended lymphadenectomy for lung cancer. *Thorac Surg* 1990;5:19–25.
7. Rusch VW, Asamura H, Watanabe H, et al. Members of IASLC Staging Committee. The IASLC lung cancer staging project: a proposal for a new international lymph node map in the forthcoming seventh edition of the TNM classification for lung cancer. *J Thorac Oncol* 2009;4:1043–1045.
8. Asamura H, Nakayama H, Kondo H, et al. Lobe-specific extent of systematic lymph node dissection for non-small cell lung carcinomas according to a retrospective study of metastasis and prognosis. *J Thorac Cardiovasc Surg* 1999;117:1102–1111.
9. Uehara H, Okumura S, Satoh Y, et al. Validity of omission of subcarinal lymph node dissection in patients with cancer of the right upper lobe or left upper division of the lung. *Jpn J Lung Cancer* 2008;48:266–272.
10. Okada M, Sakamoto T, Yuki T, et al. Border between N1 and N2 stations in lung carcinoma: lessons from lymph node metastatic patterns of lower lobe tumors. *J Thorac Cardiovasc Surg* 2008;129: 825–830.
11. Uehara H, Sakao Y, Mun M, et al. Prognostic value and significance of subcarinal and superior mediastinal lymph node metastasis in lower lobe tumours. *Eur J Cardiothorac Surg* 2010;38:498–502.
12. Ichinose Y, Kato H, Koike T, et al. Japanese Clinical Oncology Group. Completely resected stage IIIA non-small cell lung cancer: the significance of primary tumor location and N2 station. *J Thorac Cardiovasc Surg* 2001;122:803–808.
13. Sakao Y, Miyamoto H, Yamazaki A, et al. The prognostic significance of metastasis to the highest mediastinal lymph node in non-small cell lung cancer. *Ann Thorac Surg* 2006;81:292–297.
14. Naruke T, Tsuchiya R, Kondo H, et al. Lymph node sampling in lung cancer: how should it be done? *Eur J Cardiothorac Surg* 1999;16:S17–S24.

The American Journal of Pathology, Vol. 176, No. 4, April 2010

DOI: 10.2353/ajpath.2010.090500

Cell Injury, Repair, Aging and Apoptosis

Role of Insulin-Like Growth Factor Binding Protein 2 in Lung Adenocarcinoma

IGF-Independent Antiapoptotic Effect Via Caspase-3

Toshiro Migita,* Tadahito Narita,*† Reimi Asaka,* Erika Miyagi,* Hiroko Nagano,* Kimie Nomura,* Masaaki Matsuura,‡§ Yukitoshi Satoh,¶ Sakae Okumura,¶ Ken Nakagawa,¶ Hiroyuki Seimiya,‖ and Yuichi Ishikawa*

From the Divisions of Pathology, and Cancer Genomics,‡ The Cancer Institute, Tokyo; Zenyaku Kogyo Co., Ltd.,† Tokyo; the Bioinformatics Group,§ Genome Center, Tokyo; the Department of Thoracic Surgical Oncology,¶ and the Division of Molecular Biotherapy,‖ Cancer Chemotherapy Center, The Cancer Institute Hospital, Japanese Foundation for Cancer Research, Tokyo, Japan*

Insulin-like growth factor (IGF) signaling plays a pivotal role in cell proliferation and mitogenesis. Secreted IGF-binding proteins (IGFBPs) are important modulators of IGF bioavailability; however, their intracellular functions remain elusive. We sought to assess the antiapoptotic properties of intracellular IGFBP-2 in lung adenocarcinomas. IGFBP-2 overexpression resulted in a decrease in procaspase-3 expression; however, it did not influence the phosphorylation status of either IGF receptor or its downstream targets, including Akt and extracellular signal-regulated kinase. Apoptosis induced by camptothecin was significantly inhibited by IGFBP-2 overexpression in NCI-H522 cells. Conversely, selective knockdown of IGFBP-2 using small-interfering RNA resulted in an increase in procaspase-3 expression and sensitization to camptothecin-induced apoptosis in NCI-H522 cells. LY294002, an inhibitor of phosphatidylinositol 3-kinase, caused a decrease in IGFBP-2 levels and enhanced apoptosis in combination with camptothecin. Immunohistochemistry demonstrated that intracellular IGFBP-2 was highly expressed in lung adenocarcinomas compared with normal epithelium. Intracellular IGFBP-2 and procaspase-3 were expressed in a mutually exclusive manner. These findings suggest that intracellular IGFBP-2 regulates caspase-3 expression and contributes to the inhibitory effect on apoptosis independent of IGF. IGFBP-2, therefore, may offer a novel therapeutic target and serve as an antiapoptotic biomarker for lung adenocarcinoma. ***(Am J Pathol 2010, 176:1756–1766; DOI: 10.2353/ajpath.2010.090500)***

Insulin-like growth factor-I and -II (IGF-I and -II) are important regulators of cellular metabolism, growth, and survival. When IGFs bind to their receptors, the type I and type II IGF receptors (IGF-IR or IGF-IIR), they activate the downstream signaling cascades via the phosphorylation of tyrosine kinase. Activated IGF-1R transmits signals to the major distinct pathways mitogen-activated protein kinase and phosphatidyl inositol 3-kinase (PI3K), signaling pathways that are highly implicated in the development and progression of neoplasia. IGF's bioavailability is regulated by six high affinity IGF binding proteins (IGFBPs). Secreted IGFBPs by cancer cells interfere primarily with IGF-I or -II through the formation of IGF-IGFBPs complex, which in turn exert an inhibitory effect on IGF-mediated biological functions.

IGF-independent functions of extracellular IGFBPs have long been discussed. Secreted and membrane-associated IGFBP-2 directly binds to proteoglycans and integrins,[1–5] demonstrating IGFBP-2 as a negative or positive regulator of cell adhesion, migration, and invasion in an IGF-independent manner. In the same way, IGFBP-2 positively or negatively regulates cell growth

Supported by Grants-in-Aid for Scientific Research on Priority Areas from the Ministry of Education, Culture, Sports, Science, and Technology; Grants-in-Aid for Scientific Research from the Japan Society for the Promotion of Science; and by grants from the Ministry of Health, Labor, and Welfare, the National Institute of Biomedical Innovation, the Smoking Research Foundation, and the Vehicle Racing Commemorative Foundation.

Accepted for publication December 8, 2009.

Current address of T.M.: Division of Molecular Biotherapy, Cancer Chemotherapy Center, Japanese Foundation for Cancer Research, Tokyo, Japan.

Address reprint requests to Toshiro Migita, M.D., Ph.D., Division of Molecular Biotherapy, Cancer Chemotherapy Center, Japanese Foundation for Cancer Research, 3-8-31, Ariake, Koto-ku, Tokyo 135-8550, Japan. E-mail: toshiro.migita@jfcr.or.jp.

and survival in certain types of cancers *in vitro*.[2,6–11] In *in vivo* studies, the growth of mice colorectal adenomas induced by chemical carcinogen was inhibited when they were crossed with IGFBP-2 transgenic mice[12]; however, in contrast, IGFBP-2 exerts oncogenic effects in brain-specific transgenic mice.[13] Thus, increased IGFBP-2 confers advantage or disadvantage for tumor growth, depending on cell type and physiological conditions.[2,14]

Despite these two opposite effects of IGFBP-2 on biological behaviors of cancers, biochemistry and molecular pathology have demonstrated that IGFBP-2 is overexpressed in a wide variety of human malignancies, including glioma,[15] prostate cancer,[16] lung cancer,[17–19] colorectal cancer,[20] ovarian cancer,[21] adrenocortical tumor,[22] breast cancer,[23] and leukemia.[24] Importantly, IGFBP-2 is frequently overexpressed in advanced cancers and is suggested to be involved in the metastatic process.[25] Several potential mechanisms of cancer progression mediated by secreted IGFBP-2 are discussed,[14] but little study has been conducted to the analysis of intracellular-IGFBP-2 functions.

Our aim for this study is to examine the effect of intracellular IGFBP-2 on apoptosis in lung cancer cells and elucidate its molecular mechanism. We also examine the significance of intracellular IGFBP-2 and procaspase-3 in clinical samples and explore the therapeutic implications.

Materials and Methods

Cell Culture and Clinical Samples

The human lung adenocarcinoma cell lines A549, NCI-H460, NCI-H23, NCI-H522, HOP62, COR-L105, and PC14 were obtained from the American Type Culture Collection (Manassas, VA) and grown in RPMI 1640 media supplemented with 10% fetal bovine serum (both medium and serum were from Gibco-BRL, Tokyo, Japan) and 1% penicillin/streptomycin in an atmosphere of 5% CO_2 at 37°C, as previously described.[26]

We also analyzed the mRNA and protein expression in 24 pairs of primary lung adenocarcinomas and corresponding normal lung tissues. All experiments were performed by using a protocol approved by the Institutional Review Board of the Japanese Foundation for Cancer Research (number 2007-1058).

Transient and Stable Transfections

IGFBP-2 cDNA expression construct in pcDNA3.1/Neo (Invitrogen, Carlsbad, CA) was a generous gift from Dr. Hiroaki Kataoka (Section of Oncopathology and Regenerative Biology, Department of Pathology, University of Miyazaki, Japan).[27] Cells were plated at 7×10^5 per well in 60-mm dishes and transfected in triplicate by using the FuGENE 6 Transfection Reagent according to the manufacturer's protocol (Roche Diagnostics, Inc., Indianapolis, IN). We established stable cell lines COR-L105, NCI-H522, and HOP62 overexpressing IGFBP-2 after 4 weeks of selection in 400 μg/ml of neomycin.

RNA Preparation and Real-Time RT-PCR

The cells and frozen tissue were collected for RNA extraction by using an RNeasy Kit (Qiagen, Valencia, CA), and total RNA was applied for first-strand cDNA synthesis with a high capacity cDNA Reverse Transcriptase kit (Applied Biosystems, Foster City, CA). Gene-specific probes and primer were obtained from Universal Probe-Library (number 25, Roche Applied Science, Tokyo, Japan), and primer sequences were as follows: 5′-TTGCAGACAATGGCGATGACC-3′ (IGFBP-2 forward); 5′-GGGATGTGCAGGGAGTAGAGG-3′ (IGFBP-2 reverse). PCR was performed in 96-well plates by using the LightCycler 480 System (Roche Applied Science). All reactions were performed at least in triplicate. The relative amounts of all mRNAs were calculated by using the comparative threshold cycle (CT) method after normalization to human β2 microglobulin.

Cell Lysis and Immunoblotting

To obtain total protein lysates, frozen tissue and cells were homogenized and dissolved in radioimmunoprecipitation assay buffer (150 mmol/L of NaCl, 1.0% Nonidet P40, 0.5% sodium deoxycholate, 0.1% SDS, 50 mmol/L of Tris, pH 7.6) containing proteinase inhibitors and phosphatase inhibitors (Nacalai Tesque, Kyoto, Japan). The protein concentration of each lysate was determined by using a protein assay reagent kit (BioRad, Hercules, CA). The total cell lysate was applied on 4% to 12% SDS-polyacrylamide gel electrophoresis. After electrophoresis, the proteins were transferred electrophoretically from the gel to polyvinylidene difluoride membranes (Millipore, Bedford, MA). The membranes were then blocked for 1 hour in blocking buffer (5% low-fat dried milk in Tris-buffered saline) and probed with the primary antibodies overnight. After being washed, the protein content was made visible with horseradish-peroxidase-conjugated secondary antibodies followed by enhanced chemiluminescence (Amersham, Piscataway, NJ). Signal densities were quantitatively determined by ImageJ 1.36 b software (NIH, Bethesda, MD). The primary antibodies used were raised against IGFBP-2 (C-18, Santa Cruz Biotechnology, Santa Cruz, CA), caspase-3, phosphorylated (Tyr1135/1136) and total IGF-1R β, phosphorylated (Ser 473) and total Akt, phosphorylated (Thr 202/Tyr 204) and total Erk1/2, cleaved poly ADP-ribose polymerase (PARP; all obtained from Cell Signaling Technology, Danvers, MA), and β-actin (Sigma, St. Louis, MO). LY294002 was purchased from Sigma.

Caspase Activity Assay

Caspase activities were measured by using the Caspase-Glo 3/7 assay kit according to the manufacturer's instruction (Promega, Madison, WI). Cells (5×10^3 cells/well) were placed in a 96-well culture plate, followed by treatment with dimethyl sulfoxide (DMSO) vehicle or 200 nmol/L of camptothecin for 24 hours. One hundred microliters of Caspase-Glo 3/7 reagent was added to each well and incubated for 1 hour at room temperature.

The culture media with the reagent served as blank, and blank control value was subtracted from each sample value. Luminescence of all samples was measured by using a Tecan Spectrafluor Plus (Wako, Osaka, Japan).

Enzyme-Linked Immunosorbent Assay

IGFBP-2 concentrations in media of cell culture were determined with IGFBP-2 Duoset enzyme-linked immunosorbent assay (ELISA) Development system (R and D Systems, Minneapolis, MN) according to the manufacturer's protocol. Briefly, capture antibody was plated in a 96-well microplate and incubated overnight at room temperature. One hundred microliters of supernatant of culture media or IGFBP-2 standard were added into plate and incubate for 2 hours at room temperature, followed by the immunoreaction with IGFBP-2 detection antibody. IGFBP-2 concentration was calculated from the standard curve. All experiments were performed in duplicate or triplicate.

RNA Interference

Small-interfering RNA (siRNA) oligonucleotides for IGFBP-2 (Santa Cruz Biotechnology) and a negative control (Invitrogen) were transfected into the cells. Transfection was performed by using Lipofectamine RNAiMAX (Invitrogen) according to the manufacturer's protocol. Briefly, 60 pmol of siRNA and 10 μl of Lipofectamine RNAiMAX were mixed in 1 ml of Opti-MEM medium (10 nmol/L of final siRNA concentration). After 20 minutes of incubation, the mixture was added to the suspended cells and these were plated on dishes. Cells were harvested at 24-hour intervals until 72 hours after transfection.

Cell Proliferation and Apoptosis

Cell proliferation was measured as the number of viable cells, as evaluated at 450 nm optical density by using Cell Count reagent SF (Nacalai Tesque). Apoptotic cells were determined by Hoechst 33342 staining, and the apoptosis rate (percent of total population) was evaluated by counting apoptotic and nonapoptotic cells in at least three randomly selected fields.

Immunohistochemistry

Tissue microarrays were constructed from 169 paraffin-embedded lung adenocarcinomas. Briefly, H&E-stained sections containing representative tumor regions were selected. Tissues were punched from cancer areas of each donor block by using tissue cylinders with a diameter of 2 mm and then brought into a recipient paraffin block. Three tumor cores were taken per patient.

Immunohistochemistry was performed on 5-μm thick, formalin-fixed, paraffin-embedded sections by using primary antibodies for IGFBP-2 (C-18, Santa Cruz Biotechnology) and procaspase-3 (Cell Signaling Technology). Antigen retrieval was performed for 30 minutes in citrate buffer for each antibody. The slides were developed by using the labeled streptavidin biotinylated peroxidase method (Nichirei, Tokyo, Japan) according to the manufacturer's instructions. 3,3'-Diaminobenzidine tetrahydro-chloride was used as the chromogen, and hematoxylin was used as the counterstain. A549 xenografts in nude mice were previously established[26] and were used as a positive control. The primary antibody was omitted for negative controls. All immunohistochemical staining was accomplished with a Dako Autostainer (DakoCytomation, Carpenteria, CA) under the same conditions. The staining intensity of IGFBP-2 and procaspase-3 was scored semiquantitatively: positive in less than 25% of cancer cells (weak), positive in 25% to 50% of cancer cells (moderate), and positive in more than 50% of cancer cells (strong). Representative score of each patient was defined as the highest score across three cores.

Statistical Analysis

For *in vitro* experiments, statistical analysis was performed by using Welch's *t*-tests. Comparisons of IGFBP-2 mRNA levels in clinical samples were made by using paired *t*-test analysis. Dose/time dependency of drugs was determined by the confidence interval (CI) based test of slope of the linear regression. Concentrations of drugs that suppressed cell proliferation to 50% of levels exhibited by control cells (IC50) were derived from the dose-response curve. Correlation between IGFBP-2 and caspase-3 expression in immunohistochemistry was evaluated by performing the Fisher's exact test. For all analyses, $P \leq 0.05$ was considered statistically significant. Statistical analyses were performed by using the statistical programming language of R (http://www.R-project.org; accessed February 1, 2010) and Statistika (Statsoft, Inc., Tulsa, OK).

Results

IGFBP-2 Is Expressed and Secreted in Lung Adenocarcinoma Cell Lines

At first, intracellular IGFBP-2 expression levels were examined in various lung cancer cell lines by the use of Western blot. IGFBP-2 was highly expressed in A549, NCI-H460 cells, but expressed at very low levels in HOP62 and COR-L105 cells (Figure 1A).

The levels of secreted IGFBP-2 in media were measured by ELISA. Secreted IGFBP-2 levels correlated with intracellular protein levels obtained by Western blot (Figure 1B).

IGFBP-2 Expression Is Regulated Transcriptionally and Posttranslationally

IGFBP-2 expression is physiologically up-regulated by the energy restriction or insulin-dependent diabetes mellitus.[28,29] To determine whether the supplement of nutrients can alter IGFBP-2 expression in lung cancer cells, we examined the effects of glucose or serum depletion on IGFBP-2 expression in A549 cells. Glucose depletion significantly reduced IGFBP-2 levels at both protein and mRNA levels ($P = 0.0017$), whereas serum depletion did not ($P = 0.311$; Figure 2A). IGFBP-2 protein and mRNA levels were dependent on glucose concentration (Figure 2B). These findings suggest that IGFBP-2 expression in

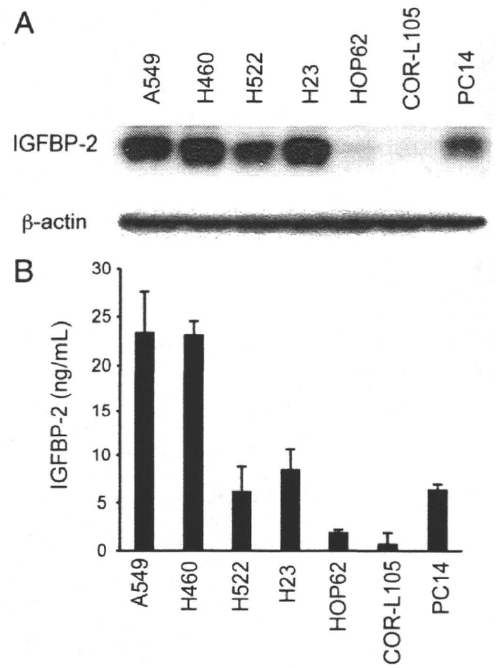

Figure 1. A: Basal levels of intracellular IGFBP-2 protein in seven lung adenocarcinoma cell lines. Cells (5×10^5) were plated in a 60-mm dish and cultured for 48 hours. The protein extracts from each cell line were resolved by SDS-polyacrylamide gel electrophoresis and blotted with an antibody against IGFBP-2. β-actin served as internal control. A representative data from two independent experiments is shown. **B:** Conditioned media containing a different amount of IGFBP-2 in lung adenocarcinoma cell lines. Secreted IGFBP-2 was measured, under the same conditions as above, by ELISA. Values represent means ± SD.

cancer cells is glucose-dependent and is regulated by a mechanism that is distinct from normal cells.

It has been reported that IGFBP-2 expression is regulated by the PI3K-PTEN (phosphatase and tensin homolog deleted on chromosome 10) pathway in prostate and glioblastoma cells.[30] Thus, extracellular and intracellular IGFBP-2 levels were evaluated in lung cancer cells treated with LY294002, a PI3K inhibitor. PTEN protein was detected in all cell lines, except PC14, as described previously.[26] Secretion of IGFBP-2 protein was suppressed in all cell lines by the treatment of LY294002 to varying degrees (Figure 2C). The effect of LY294002 on IGFBP-2 expression showed a significant dose dependence ($P = 0.0048$) and time course dependence (95% CI: 0.134 to 0.18, control; 0.029 to 0.043, LY294002) in A549 cells (Figure 2, D and E). Intracellular IGFBP-2 levels were also decreased with LY294002 (Figure 2F). Interestingly, a fraction of IGFBP-2 protein was degraded into approximately 20 kDa after treatment with LY294002 (Figure 2F). Conversely, IGFBP-2 mRNA was significantly increased with LY294002 ($P < 0.005$; Figure 2G), suggesting the existence of a compensatory feedback mechanism.

IGFBP-2 Overexpression Suppresses Procaspase-3 Expression and Confers Resistance for Drug-induced Apoptosis

To address whether IGFBP-2 is involved in apoptotic event, IGFBP-2 was enforced in cells with low endogenous IGFBP-2 levels, and then caspase expression was examined. IGFBP-2 overexpression resulted in a remarkable increase in intracellular IGFBP-2 levels in COR-L105, NCI-H522, and HOP62 cells compared with vector control (Figure 3A). Secreted IGFBP-2 levels of these cells were also increased corresponding to the levels of intracellular IGFBP-2 (Figure 3B). Intriguingly, IGFBP-2 overexpression resulted in a substantial decrease in procaspase-3 expression (Figure 3A). However, caspase-9 was not decreased (Figure 3A), suggesting IGFBP-2 specifically inhibits caspase-3 expression. Despite a higher amount of IGFBP-2 secretion into media, no significant changes were found in the IGF signaling pathway including phosphorylation statuses of IGF-1R, Akt, or Erk1/2 (Figure 3A). These findings suggest that IGFBP-2-mediated caspase-3 inhibition occurs in an IGF-independent manner.

Next, to examine whether IGFBP-2 involves in apoptotic event, we compared the sensitivity of IGFBP-2 overexpressing cells and vector control cells to an apoptosis inducer, camptothecin. IGFBP-2 overexpressing and vector control H522 cells were exposed to 20 to 1000 nmol/L of camptothecin for 24 hours, and the cell proliferation and caspase-3 activity were analyzed. The results indicated that IGFBP-2 overexpressing H522 cells were significantly resistant to camptothecin (EV, IC50 = 686 nmol/L; BP-2, IC50 > 1000 nmol/L; Figure 3C). As expected, caspase-3 activity was significantly decreased in IGFBP-2 overexpressing cells compared with vector control cells on treatment with camptothecin ($P < 0.02$; Figure 3D). Apoptosis was evaluated by Hoechst 33342 staining and PARP cleavage. Enforced IGFBP-2 significantly inhibited PARP cleavage, as determined by Western blot (Figure 3E), and reduced camptothecin-induced apoptotic cells in H522 cells ($P = 0.003$; Figure 3F). Similar results were obtained with the treatment of cisplatin or etoposide (data not shown).

IGFBP-2 Inhibition Up-Regulates Procaspase-3 Expression and Promotes Drug-Induced Apoptosis

To further elucidate the effects of IGFBP-2 on caspase-3, gene silencing for IGFBP-2 was performed in A549 and H522 cells. IGFBP-2 knockdown induced an increase in procaspase-3 expression until 72 hours after siRNA treatment in both cell lines (Figure 4A). No significant active form of cleaved caspase-3 was identified (data not shown). As is the results with IGFBP-2 overexpression, no substantial change was found in caspase-9. In addition, IGFBP-2 siRNA also decreased the phosphorylation status of IGF-1R. This effect might be because of a rapid decrease in both intracellular and extracellular IGFBP-2. Although IGFBP-2 knockdown resulted in morphological changes such as shrinkage in A549 cells, no substantial increase in apoptosis was identified by Hoechst 33342 staining or PARP cleavage (data not shown).

We now asked whether IGFBP-2 inhibition sensitizes cells for drug-induced apoptosis. Figure 4B shows the cell proliferation of IGFBP-2 knockdown and negative control cells with a treatment of camptothecin. IGFBP-2

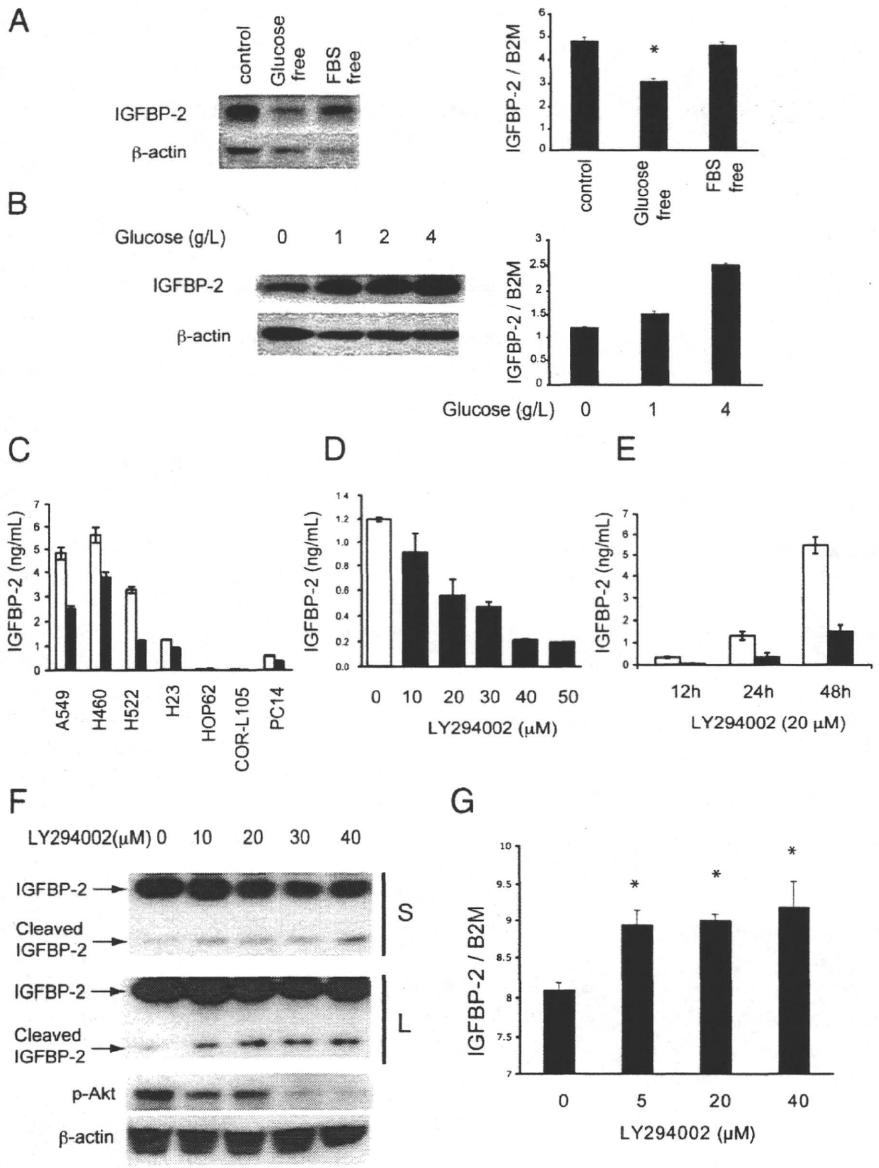

Figure 2. A: The effect of glucose and fetal bovine serum on intracellular IGFBP-2 levels. A549 cells (5×10^5) were incubated for 2 hours in fetal bovine serum (FBS) free media, followed by a 24-hour incubation in glucose free, FBS free, or regular media. The cells were then harvested and subjected to both immunoblotting and quantitative RT-PCR for IGFBP-2. IGFBP-2 mRNA was normalized to human β2 microglobulin (B2M). Values represent means ± SD. Statistical analysis was performed by Welch's *t*-test. $^*P < 0.01$. **B:** A549 cells were cultured in media with the indicated concentrations of glucose for 24 hours. IGFBP-2 expression levels were measured by both immunoblotting and quantitative RT-PCR. Values represent means ± SD. Significant slope of regression line between IGFBP-2 mRNA and glucose concentration was obtained ($P = 0.012$). **C:** Effect of LY294002, a PI3K inhibitor, on extracellular IGFBP-2 levels. Seven lung adenocarcinoma cell lines were treated either with a vehicle control DMSO (white bar) or 20 μmol/L of LY294002 (black bar) for 24 hours. Secreted IGFBP-2 was measured by ELISA as described before. **D:** A549 cells were treated with the indicated concentration of LY294002 for 24 hours. A significant slope of regression line between secreted IGFBP-2 and LY294002 concentration was obtained ($P = 0.0048$). **E:** Time course of IGFBP-2 secretion in A549 cells treated with 20 μmol/L of LY294002. The 95% CI based test of slope regression was significant ($P < 0.05$): 0.134 to 0.18 vs. 0.029 to 0.043, in control DMSO and LY294002, respectively. **F:** The effect of LY294002 on intracellular levels of IGFBP-2. A549 cells were treated with the indicated concentration of LY294002, followed by immunoblotting for IGFBP-2, phosphorylated Akt (Ser 473), and β-actin. S, short exposure; L, long exposure. **G:** A549 cells were treated with the indicated concentration of LY294002, and IGFBP-2 mRNA levels were evaluated by a real-time RT-PCR. Values represent means ± SD. Statistical analysis was performed by Welch's *t*-test. $^*P < 0.01$.

knockdown cells were more sensitive to campthothecin rather than vector control cells (95% CI: -2.7×10^{-4} to -1.6×10^{-4} vs. -4.5×10^{-4} to -3.0×10^{-4}, in negative control and IGFBP-2 siRNA, respectively; Figure 4B). In caspase-3 activity assay (Figure 4C), there were no significant changes in caspase-3 activity between negative control and IGFBP-2 siRNA with DMSO treatment (white bars). When cells were treated with camptothecin, IGFBP-2 siRNA significantly increased caspase-3 activity than negative control siRNA (black bars). The sensitivity to camptothecin was significantly potentiated by IGFBP-2 inhibition ($P < 0.0001$). Apoptosis was significantly increased in cells with IGFBP-2 siRNA compared with negative control siRNA ($P = 0.0009$; Figure 4D). Cleaved PARP was more substantial in IGFBP-2 siRNA treated cells compared with vector control H522 cells (Figure 4E). As a PI3K inhibitor induced IGFBP-2 degradation (Figure 2F), we examined whether a PI3K inhibitor has an additive effect on apoptosis with camptothecin. As expected, combination therapy of LY294002 and campthothecin enhanced PARP cleavage in H522 cells when compared with campthothecin or LY294002 alone. IGFBP-2 levels were inversely correlated with the increase in the levels of cleaved PARP (Figure 4F, left panels). In contrast, there were no substantial effects of LY294002 on PARP cleavage in COR-L105 cells, which have low IGFBP-2 levels (Figure 4F, right panels).

These data strongly suggest that IGFBP-2 regulates apoptosis via caspase-3. Moreover, IGFBP-2 becomes a therapeutic target as well as a biomarker for the treatment of PI3K inhibitors.

Tissue IGFBP-2 Is Overexpressed in Lung Adenocarcinoma

Next, we examined tissue expression levels of IGFBP-2 in human lung adenocarcinoma and normal tissue by using

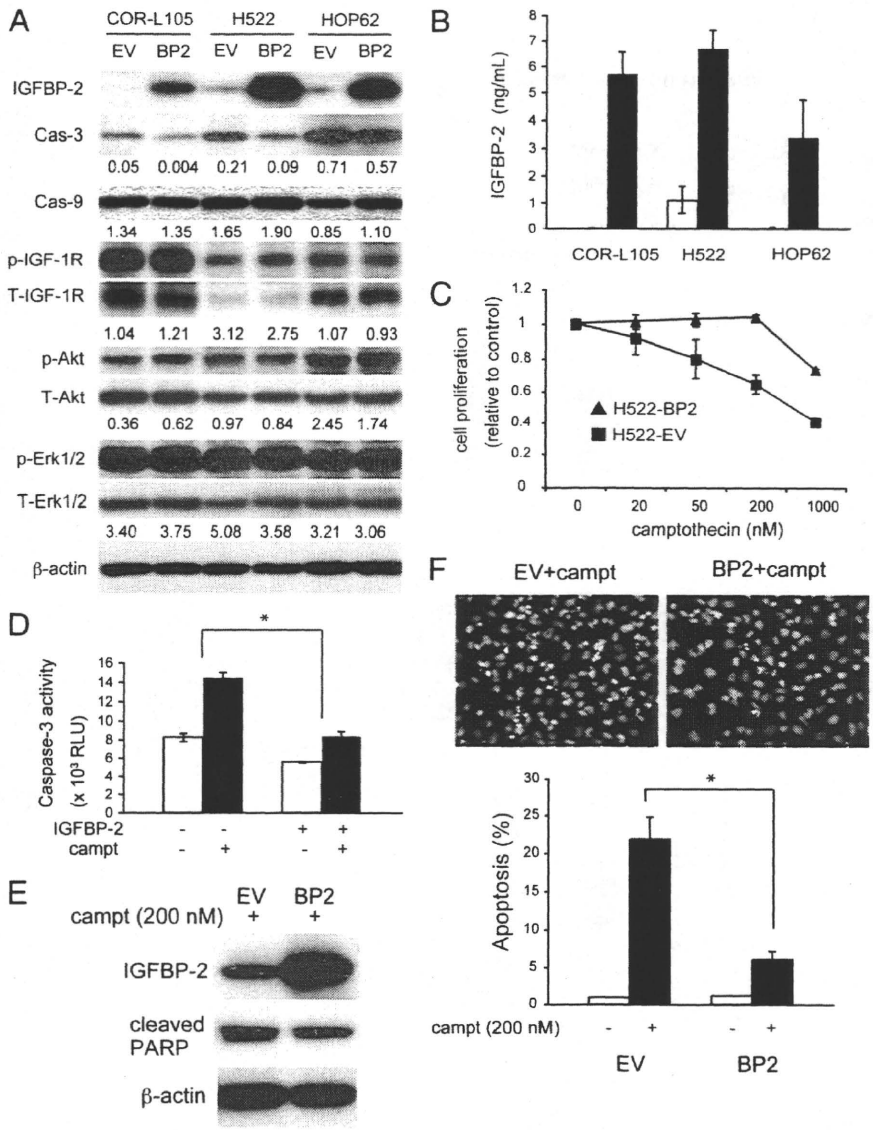

Figure 3. A: IGFBP-2 overexpression inhibits procaspase-3 expression independent of the IGF signaling pathway. Empty vector (EV) and IGFBP-2 (BP2) were transfected in COR-L105, NCI-H522, and HOP62 lung adenocarcinoma cell lines, and stably IGFBP-2 overexpressing cells were obtained. Whole cell lysates were subjected to SDS-polyacrylamide gel electrophoresis, followed by immunoblotting for IGFBP-2, procaspase-3, procaspase-9, phosphorylated and total IGF-1R, phosphorylated and total Akt, phosphorylated and total Erk1/2, and β-actin. Signal densities were quantified by ImageJ, and then procaspase-3/β-actin, procaspase-9/β-actin, p-IGF1R/T-IGF1R, p-Akt/T-Akt, and p-Erk1/2/T-Erk1/2 ratios were calculated. **B:** Secreted IGFBP-2 levels were measured by ELISA in three different stable vector- and IGFBP-2-transfected (white and black bars, respectively) cell lines. Data represent means ± SD. **C:** IGFBP-2 overexpressing and empty vector NCI-H522 cells were plated in 96 wells and treated with indicated concentration of camptothecin for 24 hours. Cell proliferation was determined by microplate reader using cell count reagent. Data represent means ± SD. The IC50 values were 686 nmol/L and more than 1000 nmol/L in empty vector and IGFBP-2 cells, respectively. **D:** Caspase-3 assay in IGFBP-2 overexpressing and empty vector NCI-H522 cells. Cells were plated in 96 wells and treated with 200 nmol/L of camptothecin for 24 hours. Caspase-3 activity was determined by a microplate reader. Data represent means ± SD. Statistical analysis of comparison between empty vector and IGFBP-2 overexpressing cells was performed by Welch's *t*-test. EV (camptothecin/DMSO) versus BP2 (camptothecin/DMSO); $^*P < 0.02$. **E:** Apoptosis was also evaluated by immunoblotting for PARP cleavage with whole cell lysate. **F:** Twenty-four hours after exposure of 200 nmol/L of camptothecin, cells were stained with Hoechst 33342. Apoptotic and nonapoptotic cells were counted by microscopy at least in three different areas, and the apoptotic rate was represented. Values represent means ± SD. Statistical analysis was performed by Welch's *t*-test. $^*P < 0.01$.

a real-time RT-PCR and Western blotting. IGFBP-2 mRNA was significantly higher in tumors than in paired normal tissue, as examined by a real-time RT-PCR ($P = 0.021$; Figure 5A). A higher amount of IGFBP-2 protein was also frequently observed in tumor tissue compared with in paired normal tissue (Figure 5B).

Inverse Relationship between IGFBP-2 and Caspase-3 Expression

Finally, immunohistochemical analysis was performed on tissue microarray including 169 cases of lung adenocarcinoma. IGFBP-2 expression was mostly confined to cancer cells, whereas normal lung epithelium revealed very low or undetectable IGFBP-2 levels (Figure 6A, arrowheads). In most cases, IGFBP-2 was localized in cytoplasm of lung adenocarcinoma cells, as shown in Figure 6A. Membraneous IGFBP-2 expression was found in only 3 of 169 cases (1.8%; Figure 6B). IGFBP-2 was expressed in early precursor lesions, and its expression levels increased gradually as the lesions progress from benign (Figure 6C, arrows) to malignant cells (Figure 6C, arrowheads). In particular, a strong IGFBP-2 expression was found in cancer cells with high nuclear grade distinct from ones with low nuclear grade even within the same gland (Figure 6D). It should be noted that the mutually exclusive expression between IGFBP-2 (Figure 6E, left panel, arrowheads and Figure 6F, left panel, upper area) and procaspase-3 (Figure 6E, right panel, arrowheads and Figure 6F, right panel, lower area) was frequently observed in lung adenocarcinomas. To summarize the immunohistochemical data, a significant inverse correlation between the groups in the numbers of patients with IGFBP-2 and procaspase-3 expression was observed in lung adenocarcinomas (Table 1).

Discussion

The IGF signaling pathway plays a pivotal role in cellular proliferation, differentiation, survival, and metabolism.

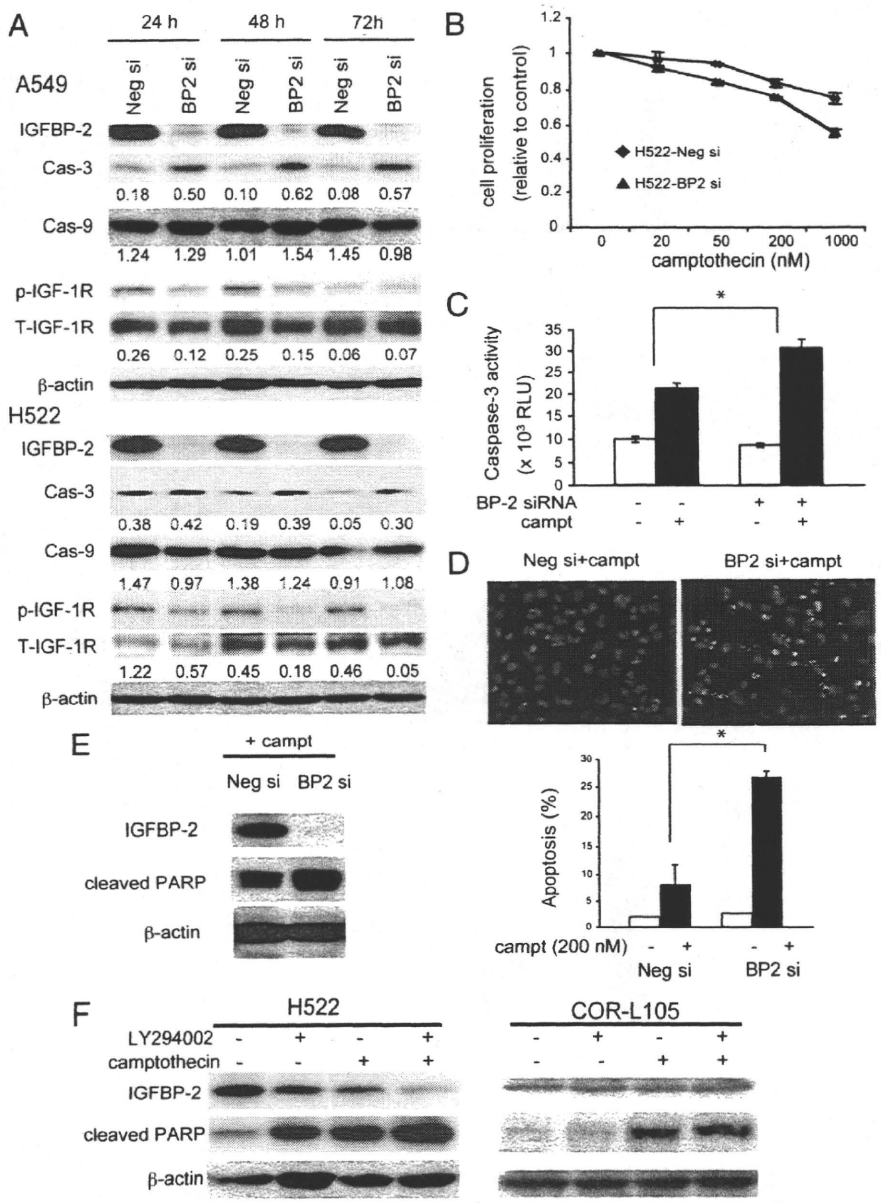

Figure 4. A: Specific IGFBP-2 inhibition resulted in the increase in procaspase-3. A549 or NCI-H522 cells were transfected with negative control or IGFBP-2 siRNA oligonucleotides, followed by immunoblot for IGFBP-2, procaspase-3, procaspase-9, phosphorylated and total IGF-1R, and β-actin at indicated times after transfection. Signal densities were quantified by ImageJ, and then procaspase-3/β-actin, Procaspase-9/β-actin, and p-IGF1R/T-IGF1R ratios were calculated. **B:** NCI-H522 cells were treated with negative control or IGFBP-2 siRNA for 24 hours and then exposed to different concentrations of camptothecin for 24 hours. Cell proliferation was determined as described before. Data represent means ± SD. A 95% CI based test of slope regression was significant ($P < 0.05$): −2.7E-04 to −1.6E-04 in negative siRNA vs. −4.5E-04 to −3.0E-04 in IGFBP-2 siRNA. **C:** Caspase-3 assay in NCI-H522 cells treated with negative control or IGFBP-2 siRNA. NCI-H522 cells were treated with negative control or IGFBP-2 siRNA for 48 hours in 96 wells and then treated with 200 nmol/L of camptothecin for 24 hours. Caspase-3 activity was determined by a microplate reader. Data represent means ± SD. Statistical analysis of comparison between negative control and IGFBP-2 siRNA was performed by Welch's *t*-test. $^*P < 0.0001$. **D:** Twenty-four hours after exposure of 200 nmol/L of camptothecin, siRNA-treated NCI-H522 cells were stained with Hoechst 33342. The apoptotic rate was measured as described previously. Values represent means ± SD. Statistical analysis was performed by Welch's *t*-test. $^*P < 0.001$. **E:** Apoptosis was also evaluated by immunoblot for PARP cleavage in NCI-H522 cells. **F:** NCI-H522 and COR-L105 cells were treated with 20 μmol/L of LY294002 or 200 nmol/L of camptothecin or combination of LY294002 and camptothecin for 24 hours. Immunoblot was performed with IGFBP-2, cleaved PARP, and β-actin antibodies.

IGFBPs are circulating proteins and function as modulators of IGF signaling through sequestration of IGFs in serum and the extracellular fluid. Increased levels of serum IGFBP-2 are found in certain pathophysiological conditions including fasting, diabetes mellitus, growth hormone deficiency, hepatic or renal failure, and cancer.[31] In cancer, IGFBP-2 exerts various biological functions by virtue of IGF-dependent or -independent mechanisms. Soluble IGFBP-2 binds to IGFs and consequently inhibits IGF signaling in various human cancers, including lung cancer.[19,32–34] Membrane-associated IGFBP-2 stimulates or inhibits cell proliferation and migration through a direct binding to serum and extracellular matrix molecules, such as cell surface integrin receptors, proteoglycans, and heparin.[2–5,35] Meanwhile, a number of studies demonstrate that intracellular IGFBP-2 promotes cancer cell growth in various cell types.[9,11,36] Moreover, IGFBP-2 overexpression confers resistance to apoptosis induced by chemotherapy in breast cancer cells[6] and by androgen ablation in prostate cancer.[9] Serum IGFBP-2 can be used for prediction of chemotherapy response and prognosis in ovarian cancer[37] and acute lymphoblastic leukemia.[38] Notably, IGFBP-2 is a marker for antiestrogen resistance, but not for cell growth in human breast cancer cells.[39] These observations invoke that intracellular IGFBP-2 mainly contributes to cancer cell survival independently of secreted IGFBP-2.

In the present study, we have shown that (1) intracellular IGFBP-2 regulates caspase-3 expression in an IGF independent manner; (2) IGFBP-2 overexpression prevents camptothecin-induced apoptosis, whereas IGFBP-2 inhibition promotes apoptosis; and (3) there is an inverse expression pattern between intracellular IGFBP-2 and caspase-3 in human lung adenocarcinomas.

We demonstrated a novel mechanism of antiapoptotic effect of IGFBP-2 via procaspase-3 inhibition in lung can-

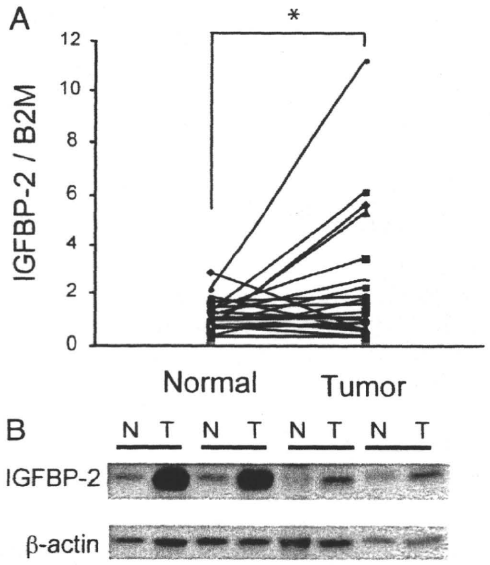

Figure 5. A: IGFBP-2 mRNA expression was measured by real-time RT-PCR in 24 pairs of human normal and corresponding tumor tissue. The mRNA levels of IGFBP-2 are presented as arbitrary units for the mRNA levels of human β2 microglobulin (B2M). A paired *t*-test was used for statistical significance (*P = 0.021). **B:** Representative picture of Western blots. IGFBP-2 protein levels were measured with four pairs of normal (N) and corresponding tumor (T) tissue from lung adenocarcinoma patients.

cer. Caspases are cysteine proteases that play essential roles in mammalian apoptosis. Procaspase-3 cleavage and consequent activation is the final step of caspase cascades in response to various apoptotic stimuli. Several authors have proved that enforced procaspase-3 potentiates sensitivity to chemotherapy and promotes apoptosis.[40–42] In lung cancer, decreased caspase-3 expression has been shown as a poorer prognostic factor in non-small-cell lung cancer.[43–45]

Our results raise the important question regarding the regulatory mechanisms involved in caspase-3 inhibition via IGFBP-2. A recent report has shown that transcriptional factor Sp1 activates the caspase-3 promoter.[46] Mammalian IGFBP-2 also has the Sp1 binding regions upstream of the transcriptional start site.[47] One possible explanation for the regulation of caspase-3 via IGFBP-2 is that IGFBP-2 overexpression in cancer cells inhibits Sp1 through negative feedback mechanism, and thereby inhibits caspase-3 gene and protein expression. Another possibility is PTEN. IGFBP-2 has been identified as the most significant molecular signature for loss of PTEN in brain and prostate cancer.[30] It has been shown that PTEN is cleaved by caspase-3 in a PTEN phosphorylation-regulated manner.[48] IGFBP-2 overexpression may induce PTEN up-regulation and protein stabilization through feedback mechanisms, and thereby negatively regulating caspase-3 activation. Future studies will help to identify the precise regulatory mechanism of caspase-3 mediated by IGFBP-2. Recent studies demonstrate caspase-3 has apoptosis-independent physiological functions, including differentiation, maturation, proliferation, and immuno response.[49,50] Thus, caspase-3 may contribute to lung cancer development and progression by multiple functions including apoptosis.

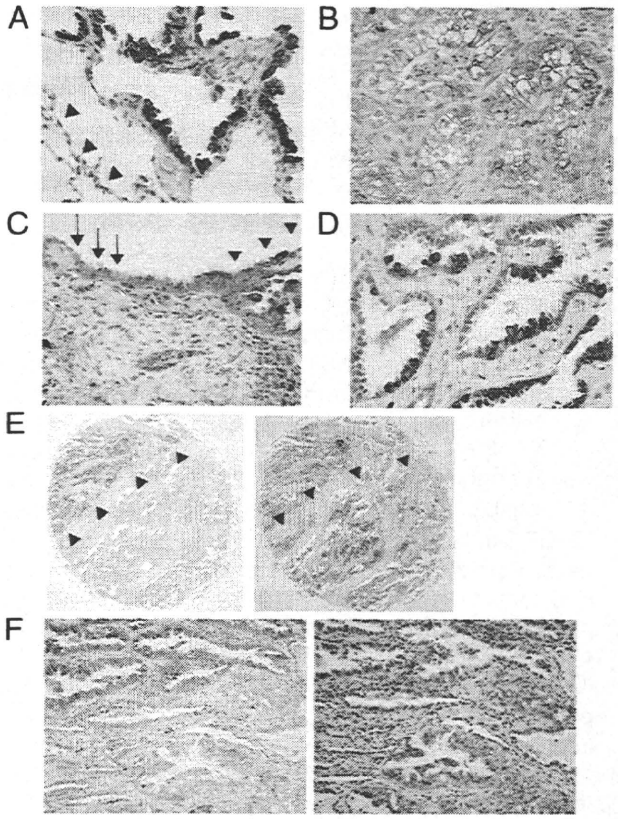

Figure 6. A: Representative pictures of immunohistochemistry for IGFBP-2 in lung adenocarcinomas. Note a strong immunoreactivity in cytoplasm of cancer cells, whereas almost negligible in normal epithelium (**arrowheads**). **B:** Typical membraneous IGFBP-2 expression. **C:** IGFBP-2 expression is gradually increased from benign cells (**arrows**) to malignant cells (**arrowheads**). **D:** Strong IGFBP-2 expression is only localized in cancer cells with high nuclear grade. **E:** Representative mutually exclusive expression between IGFBP-2 (**left**, **arrowheads**) and procaspase-3 (**right**, **arrowheads**) in serial sections on tissue microarray. **F:** Another case also demonstrates an inverse expression pattern between IGFBP-2 (**left**) and procaspase-3 (**right**) in serial sections. Original magnification: ×400 (**A–D**, and **F**); ×100 (**E**).

Because IGF signaling was not altered by the overexpression of intracellular IGFBP-2, our data suggest that intracellular and secreted IGFBP-2 are functionally independent. Interestingly, IGFBP-5 is another cancer-associated IGFBP, and it has been reported that intracellular IGFBP-5 induces growth inhibition and caspase-dependent apoptosis of breast cancer cells, whereas adding secreted-IGFBP-5 was not internalized and had no effects on growth and apoptosis.[51] Further, endogenous and exogenous IGFBP-5 is suggested to exhibit opposing actions on cell survival in osteosarcoma cells.[52] IGFBP-3, a most major IGFBP in serum, also induces

Table 1. Inverse Relationship between IGFBP-2 and Caspase-3 Expression in 169 Cases of Lung Adenocarcinomas

	Caspase-3		
IGFBP-2	Weak	Moderate	Strong
Weak	48	20	10
Moderate	40	9	2
Strong	40	0	0

Fisher's exact test was used for statistical significance (P = 0.0002). Data represent the number of patients.

growth inhibition and apoptosis in cancer cells, but it does not require the cell surface binding and nuclear translocation of IGFBP-3 in breast and prostate cancer.[53,54] These lines of evidence prompt us to propose that intracellular IGFBP-2 elicits antiapoptosis effects on cancer cells via intracrine mechanism, independent of secreted IGFBP-2. Although not yet identified in IGFBP-2, the posttranslational modification (ie, glycosylation) of secreted IGFBP-3 or -5 can be involved in the functional difference between intracellular and secreted form.[51]

There are a number of lines of evidence that IGFBP-3 is able to induce apoptosis and potentiate the apoptotic effects of UV or chemotherapy.[55,56] The inverse relationship between IGFBP-2 and IGFBP-3 expression at tissue and serum levels in a variety of cancers, including prostate,[31,55,57] ovarian,[58] and testicular cancer, has been well recognized.[59] We also found a relatively inverse relationship between secreted levels of IGFBP-2 and IGFBP-3 in lung adenocarcinoma cell lines (unpublished data). Remarkably, IGFBP-2 is predominantly expressed in cytoplasm and nucleus of lung epithelium when exposed to hyperoxia, whereas IGFBP-3 is localized in the extracellular compartment.[60] These findings suggest that IGFBP-2 and -3 may be differentially regulated and also exert a distinct action for cell proliferation and apoptosis in different compartments.

Our immunohistochemical analysis demonstrated that most adenocarcinomas revealed a cytoplasmic IGFBP-2 expression pattern, and a significant inverse association between IGFBP-2 and procaspase-3 expression. These results support the evidence that intracellular IGFBP-2 regulates procaspase-3 expression *in vitro*, thereby inhibiting apoptosis. Interestingly, IGFBP-2 expression showed a marked heterogeneity within lung adenocarcinoma tissue. At cellular levels, a strong IGFBP-2 expression was found in cancer cells having high nuclear grade. This finding suggests IGFBP-2 overexpression in cancer cells is caused by adaptive mechanisms in tumor microenvironment and confers aggressive biological nature to survive under the toxic conditions.

IGFBP-2 protein is degraded by proteases such as matrix metalloprotease-1 and -7, calpain, as well as by basic fibroblast growth factor and an androgen blockade.[61–64] We found IGFBP-2 protein was degraded by a treatment of PI3K inhibitor in A549 cells. Because a various new PI3K inhibitors have been entered clinical trials,[65] IGFBP-2 would be a useful biomarker for the treatment with PI3K inhibitors in lung cancer as well as in glioma, prostate, and breast cancers.[30,66] Further, our results suggested that IGFBP-2 is a therapeutic target in lung cancer, in line with the results in breast and ovarian cancers.[6,10] In general, lung adenocarcinomas typically showed a resistance to multiple cancer chemotherapy. Because cytoplasmic IGFBP-2 may provide cancer cells with an antiapoptotic ability, IGFBP-2 is an attractive therapeutic target especially for chemotherapy resistant tumors. The combination of chemotherapy and the IGFBP-2 or PI3K inhibitors may also potentiate drug-sensitivity.

Lung cancer is the leading cause of cancer death worldwide. Despite the availability of some cytotoxins and molecular target therapy, the efficacy of these agents is limited. It has thus become increasingly necessary to identify novel approaches to treat lung cancer. We propose that IGFBP-2 is not only a useful biomarker for predicting chemotherapy response, but also a novel therapeutic target in lung cancer.

Acknowledgments

We thank Ms. Tomoyo Kakita, Ms. Mayumi Ogawa, and Mr. Hironori Murayama for their excellent technical assistance, and Dr. Hiroaki Kataoka for IGFBP-2 constructs. We also thank Dr. Farid Gizatullin for helpful discussion.

References

1. Pereira JJ, Meyer T, Docherty SE, Reid HH, Marshall J, Thompson EW, Rossjohn J, Price JT: Bimolecular interaction of insulin-like growth factor (IGF) binding protein-2 with alphavbeta3 negatively modulates IGF-I-mediated migration and tumor growth. Cancer Res 2004, 64:977–984
2. Wang GK, Hu L, Fuller GN, Zhang W: An interaction between insulin-like growth factor-binding protein 2 (IGFBP2) and integrin alpha5 is essential for IGFBP2-induced cell mobility. J Biol Chem 2006, 281:14085–14091
3. Russo VC, Bach LA, Fosang AJ, Baker NL, Werther GA: Insulin-like growth factor binding protein-2 binds to cell surface proteoglycans in the rat brain olfactory bulb. Endocrinology 1997, 138:4858–4867
4. Schutt BS, Langkamp M, Rauschnabel U, Ranke MB, Elmlinger MW: Integrin-mediated action of insulin-like growth factor binding protein-2 in tumor cells. J Mol Endocrinol 2004, 32:859–868
5. Firth SM, Baxter RC: Cellular actions of the insulin-like growth factor binding proteins. Endocr Rev 2002, 23:824–854
6. So AI, Levitt RJ, Eigl B, Fazli L, Muramaki M, Leung S, Cheang MC, Nielsen TO, Gleave M, Pollak M: Insulin-like growth factor binding protein-2 is a novel therapeutic target associated with breast cancer. Clin Cancer Res 2008, 14:6944–6954
7. Wang H, Wang H, Shen W, Huang H, Hu L, Ramdas L, Zhou YH, Liao WS, Fuller GN, Zhang W: Insulin-like growth factor binding protein 2 enhances glioblastoma invasion by activating invasion-enhancing genes. Cancer Res 2003, 63:4315–4321
8. Miyake H, Hara I, Yamanaka K, Muramaki M, Gleave M, Eto H: Introduction of insulin-like growth factor binding protein-2 gene into human bladder cancer cells enhances their metastatic potential. Oncol Rep 2005, 13:341–345
9. Kiyama S, Morrison K, Zellweger T, Akbari M, Cox M, Yu D, Miyake H, Gleave ME: Castration-induced increases in insulin-like growth factor-binding protein 2 promotes proliferation of androgen-independent human prostate LNCaP tumors. Cancer Res 2003, 63:3575–3584
10. Lee EJ, Mircean C, Shmulevich I, Wang H, Liu J, Niemisto A, Kavanagh JJ, Lee JH, Zhang W: Insulin-like growth factor binding protein 2 promotes ovarian cancer cell invasion. Mol Cancer 2005, 4:7
11. Hoeflich A, Fettscher O, Lahm H, Blum WF, Kolb HJ, Engelhardt D, Wolf E, Weber MM: Overexpression of insulin-like growth factor-binding protein-2 results in increased tumorigenic potential in Y-1 adrenocortical tumor cells. Cancer Res 2000, 60:834–838
12. Diehl D, Hessel E, Oesterle D, Renner-Muller I, Elmlinger M, Langhammer M, Gottlicher M, Wolf E, Lahm H, Hoeflich A: IGFBP-2 overexpression reduces the appearance of dysplastic aberrant crypt foci and inhibits growth of adenomas in chemically induced colorectal carcinogenesis. Int J Cancer 2009, 124:2220–2225
13. Dunlap SM, Celestino J, Wang H, Jiang R, Holland EC, Fuller GN, Zhang W: Insulin-like growth factor binding protein 2 promotes glioma development and progression. Proc Natl Acad Sci USA: 2007, 104:11736–11741
14. Hoeflich A, Reisinger R, Lahm H, Kiess W, Blum WF, Kolb HJ, Weber MM, Wolf E: Insulin-like growth factor-binding protein 2 in tumorigenesis: protector or promoter? Cancer Res 2001, 61:8601–8610
15. Fuller GN, Rhee CH, Hess KR, Caskey LS, Wang R, Bruner JM, Yung WK, Zhang W: Reactivation of insulin-like growth factor binding pro-

tein 2 expression in glioblastoma multiforme a revelation by parallel gene expression profiling. Cancer Res 1999, 59:4228–4232
16. Kanety H, Madjar Y, Dagan Y, Levi J, Papa MZ, Pariente C, Goldwasser B, Karasik A: Serum insulin-like growth factor-binding protein-2 (IGFBP-2) is increased and IGFBP-3 is decreased in patients with prostate cancer: correlation with serum prostate-specific antigen. J Clin Endocrinol Metab 1993, 77:229–233
17. Lee DY, Kim SJ, Lee YC: Serum insulin-like growth factor (IGF)-I and IGF-binding proteins in lung cancer patients. J Korean Med Sci 1999, 14:401–404
18. Yazawa T, Sato H, Shimoyamada H, Okudela K, Woo T, Tajiri M, Ogura T, Ogawa N, Suzuki T, Mitsui H, Ishii J, Miyata C, Sakaeda M, Goto K, Kashiwagi K, Masuda M, Takahashi T, Kitamura H: Neuroendocrine cancer-specific up-regulating mechanism of insulin-like growth factor binding protein-2 in small cell lung cancer. Am J Pathol 2009, 175:976–987
19. Sato H, Yazawa T, Suzuki T, Shimoyamada H, Okudela K, Ikeda M, Hamada K, Yamada-Okabe H, Yao M, Kubota Y, Takahashi T, Kamma H, Kitamura H: Growth regulation via insulin-like growth factor binding protein-4 and -2 in association with mutant K-ras in lung epithelia. Am J Pathol 2006, 169:1550–1566
20. el Atiq F, Garrouste F, Remacle-Bonnet M, Sastre B, Pommier G: Alterations in serum levels of insulin-like growth factors and insulin-like growth-factor-binding proteins in patients with colorectal cancer. Int J Cancer 1994, 57:491–497
21. Karasik A, Menczer J, Pariente C, Kanety H: Insulin-like growth factor-I (IGF-I) and IGF-binding protein-2 are increased in cyst fluids of epithelial ovarian cancer. J Clin Endocrinol Metab 1994, 78:271–276
22. Boulle N, Logie A, Gicquel C, Perin L, Le Bouc Y: Increased levels of insulin-like growth factor II (IGF-II) and IGF-binding protein-2 are associated with malignancy in sporadic adrenocortical tumors. J Clin Endocrinol Metab 1998, 83:1713–1720
23. Busund LT, Richardsen E, Busund R, Ukkonen T, Bjornsen T, Busch C, Stalsberg H: Significant expression of IGFBP2 in breast cancer compared with benign lesions. J Clin Pathol 2005, 58:361–366
24. Mohnike KL, Kluba U, Mittler U, Aumann V, Vorwerk P, Blum WF: Serum levels of insulin-like growth factor-I, -II and insulin-like growth factor binding proteins -2 and -3 in children with acute lymphoblastic leukaemia. Eur J Pediatr 1996, 155:81–86
25. DeGraff DJ, Aguiar AA, Sikes RA: Disease evidence for IGFBP-2 as a key player in prostate cancer progression and development of osteosclerotic lesions. Am J Transl Res 2009, 1:115–130
26. Migita T, Narita T, Nomura K, Miyagi E, Inazuka F, Matsuura M, Ushijima M, Mashima T, Seimiya H, Satoh Y, Okumura S, Nakagawa K, Ishikawa Y: ATP citrate lyase: activation and therapeutic implications in non-small cell lung cancer. Cancer Res 2008, 68:8547–8554
27. Fukushima T, Tezuka T, Shimomura T, Nakano S, Kataoka H: Silencing of insulin-like growth factor-binding protein-2 in human glioblastoma cells reduces both invasiveness and expression of progression-associated gene CD24. J Biol Chem 2007, 282:18634–18644
28. Rajaram S, Baylink DJ, Mohan S: Insulin-like growth factor-binding proteins in serum and other biological fluids: regulation and functions. Endocr Rev 1997, 18:801–831
29. Kaaks R, Lukanova A: Energy balance and cancer: the role of insulin and insulin-like growth factor-I Proc Nutr Soc 2001, 60:91–106
30. Mehrian-Shai R, Chen CD, Shi T, Horvath S, Nelson SF, Reichardt JK, Sawyers CL: Insulin growth factor-binding protein 2 is a candidate biomarker for PTEN status and PI3K/Akt pathway activation in glioblastoma and prostate cancer. Proc Natl Acad Sci USA 2007, 104:5563–5568
31. Blum WF, Horn N, Kratzsch J, Jorgensen JO, Juul A, Teale D, Mohnike K, Ranke MB: Clinical studies of IGFBP-2 by radioimmunoassay. Growth Regul 1993, 3:100–104
32. Reeve JG, Morgan J, Schwander J, Bleehen NM: Role for membrane and secreted insulin-like growth factor-binding protein-2 in the regulation of insulin-like growth factor action in lung tumors. Cancer Res 1993, 53:4680–4685
33. Grimberg A, Coleman CM, Shi Z, Burns TF, MacLachlan TK, Wang W, El-Deiry WS: Insulin-like growth factor binding protein-2 is a novel mediator of p53 inhibition of insulin-like growth factor signaling. Cancer Biol Ther 2006, 5:1408–1414
34. Lukanova A, Toniolo P, Akhmedkhanov A, Biessy C, Haley NJ, Shore RE, Riboli E, Rinaldi S, Kaaks R: A prospective study of insulin-like growth factor-I, IGF-binding proteins-1, -2 and -3 and lung cancer risk in women. Int J Cancer 2001, 92:888–892
35. Kuang Z, Yao S, Keizer DW, Wang CC, Bach LA, Forbes BE, Wallace JC, Norton RS: Structure, dynamics and heparin binding of the C-terminal domain of insulin-like growth factor-binding protein-2 (IGFBP-2). J Mol Biol 2006, 364:690–704
36. Moore MG, Wetterau LA, Francis MJ, Peehl DM, Cohen P: Novel stimulatory role for insulin-like growth factor binding protein-2 in prostate cancer cells. Int J Cancer 2003, 105:14–19
37. Baron-Hay S, Boyle F, Ferrier A, Scott C: Elevated serum insulin-like growth factor binding protein-2 as a prognostic marker in patients with ovarian cancer. Clin Cancer Res 2004, 10:1796–1806
38. Vorwerk P, Mohnike K, Wex H, Rohl FW, Zimmermann M, Blum WF, Mittler U: Insulin-like growth factor binding protein-2 at diagnosis of childhood acute lymphoblastic leukemia and the prediction of relapse risk. J Clin Endocrinol Metab 2005, 90:3022–3027
39. Juncker-Jensen A, Lykkesfeldt AE, Worm J, Ralfkiaer U, Espelund U, Jepsen JS: Insulin-like growth factor binding protein 2 is a marker for antiestrogen resistant human breast cancer cell lines but is not a major growth regulator. Growth Horm IGF Res 2006, 16:224–239
40. Miyoshi N, Naniwa K, Kumagai T, Uchida K, Osawa T, Nakamura Y: Alpha-tocopherol-mediated caspase-3 up-regulation enhances susceptibility to apoptotic stimuli. Biochem Biophys Res Commun 2005, 334:466–473
41. Yang XH, Sladek TL, Liu X, Butler BR, Froelich CJ, Thor AD: Reconstitution of caspase 3 sensitizes MCF-7 breast cancer cells to doxorubicin- and etoposide-induced apoptosis. Cancer Res 2001, 61:348–354
42. Friedrich K, Wieder T, Von Haefen C, Radetzki S, Janicke R, Schulze-Osthoff K, Dorken B, Daniel PT: Overexpression of caspase-3 restores sensitivity for drug-induced apoptosis in breast cancer cell lines with acquired drug resistance. Oncogene 2001, 20:2749–2760
43. Saad AG, Yeap BY, Thunnissen FB, Pinkus GS, Pinkus JL, Loda M, Sugarbaker DJ, Johnson BE, Chirieac LR: Immunohistochemical markers associated with brain metastases in patients with non-small-cell lung carcinoma. Cancer 2008, 113:2129–2138
44. Yoo J, Jung JH, Lee MA, Seo KJ, Shim BY, Kim SH, Cho DG, Ahn MI, Kim CH, Cho KD, Kang SJ, Kim HK: Immunohistochemical analysis of non-small cell lung cancer: correlation with clinical parameters and prognosis. J Korean Med Sci 2007, 22:318–325
45. Koomagi R, Volm M: Relationship between the expression of caspase-3 and the clinical outcome of patients with non-small cell lung cancer. Anticancer Res 2000, 20:493–496
46 Sudhakar C, Jain N, Swarup G: Sp1-like sequences mediate human caspase-3 promoter activation by p73 and cisplatin. Febs J 2008, 275:2200–2213
47. Kutoh E, Margot JB, Schwander J: Identification and characterization of the putative retinoblastoma control element of the rat insulin-like growth factor binding protein-2 gene. Cancer Lett 1999, 136:187–194
48. Torres J, Rodriguez J, Myers MP, Valiente M, Graves JD, Tonks NK, Pulido R: Phosphorylation-regulated cleavage of the tumor suppressor PTEN by caspase-3: implications for the control of protein stability and PTEN-protein interactions. J Biol Chem 2003, 278:30652–30660
49. Kuranaga E, Miura M: Nonapoptotic functions of caspases: caspases as regulatory molecules for immunity and cell-fate determination. Trends Cell Biol 2007, 17:135–144
50. Nhan TQ, Liles WC, Schwartz SM: Physiological functions of caspases beyond cell death. Am J Pathol 2006, 169:729–737
51. Butt AJ, Dickson KA, McDougall F, Baxter RC: Insulin-like growth factor-binding protein-5 inhibits the growth of human breast cancer cells in vitro and in vivo. J Biol Chem 2003, 278:29676–29685
52. Yin P, Xu Q, Duan C: Paradoxical actions of endogenous and exogenous insulin-like growth factor-binding protein-5 revealed by RNA interference analysis. J Biol Chem 2004, 279:32660–32666
53. Bhattacharyya N, Pechhold K, Shahjee H, Zappala G, Elbi C, Raaka B, Wiench M, Hong J, Rechler MM: Nonsecreted insulin-like growth factor binding protein-3 (IGFBP-3) can induce apoptosis in human prostate cancer cells by IGF-independent mechanisms without being concentrated in the nucleus. J Biol Chem 2006, 281:24588–24601
54. Butt AJ, Fraley KA, Firth SM, Baxter RC: IGF-binding protein-3-induced growth inhibition and apoptosis do not require cell surface binding and nuclear translocation in human breast cancer cells. Endocrinology 2002, 143:2693–2699
55. Nickerson T, Huynh H, Pollak M: Insulin-like growth factor binding

protein-3 induces apoptosis in MCF7 breast cancer cells. Biochem Biophys Res Commun 1997, 237:690–693
56. Rajah R, Valentinis B, Cohen P: Insulin-like growth factor (IGF)-binding protein-3 induces apoptosis and mediates the effects of transforming growth factor-beta1 on programmed cell death through a p53- and IGF-independent mechanism. J Biol Chem 1997, 272:12181–12188
57. Tennant MK, Thrasher JB, Twomey PA, Birnbaum RS, Plymate SR: Insulin-like growth factor-binding protein-2 and -3 expression in benign human prostate epithelium, prostate intraepithelial neoplasia, and adenocarcinoma of the prostate. J Clin Endocrinol Metab 1996, 81:411–420
58. Flyvbjerg A, Mogensen O, Mogensen B, Nielsen OS: Elevated serum insulin-like growth factor-binding protein 2 (IGFBP-2) and decreased IGFBP-3 in epithelial ovarian cancer: correlation with cancer antigen 125 and tumor-associated trypsin inhibitor. J Clin Endocrinol Metab 1997, 82:2308–2313
59. Fottner C, Sattarova S, Hoffmann K, Spottl G, Weber MM: Elevated serum levels of IGF-binding protein 2 in patients with non-seminomatous germ cell cancer: correlation with tumor markers alpha-fetoprotein and human chorionic gonadotropin. Eur J Endocrinol 2008, 159:317–327
60. Besnard V, Corroyer S, Trugnan G, Chadelat K, Nabeyrat E, Cazals V, Clement A: Distinct patterns of insulin-like growth factor binding protein (IGFBP)-2 and IGFBP-3 expression in oxidant exposed lung epithelial cells. Biochim Biophys Acta 2001, 1538:47–58
61. Berg U, Bang P, Carlsson-Skwirut C: Calpain proteolysis of insulin-like growth factor binding protein (IGFBP) -2 and -3, but not of IGFBP-1. Biol Chem 2007, 388:859–863
62. Nakamura M, Miyamoto S, Maeda H, Ishii G, Hasebe T, Chiba T, Asaka M, Ochiai A: Matrix metalloproteinase-7 degrades all insulin-like growth factor binding proteins and facilitates insulin-like growth factor bioavailability. Biochem Biophys Res Commun 2005, 333:1011–1016
63. DeGraff DJ, Malik M, Chen Q, Miyako K, Rejto L, Aguiar AA, Bancroft DR, Cohen P, Sikes RA: Hormonal regulation of IGFBP-2 proteolysis is attenuated with progression to androgen insensitivity in the LNCaP progression model. J Cell Physiol 2007, 213:261–268
64. Russo VC, Rekaris G, Baker NL, Bach LA, Werther GA: Basic fibroblast growth factor induces proteolysis of secreted and cell membrane-associated insulin-like growth factor binding protein-2 in human neuroblastoma cells. Endocrinology 1999, 140:3082–3090
65. Yap TA, Garrett MD, Walton MI, Raynaud F, de Bono JS, Workman P: Targeting the PI3K-AKT-mTOR pathway: progress, pitfalls, and promises. Curr Opin Pharmacol 2008, 8:393–412
66. Martin JL, Baxter RC: Expression of insulin-like growth factor binding protein-2 by MCF-7 breast cancer cells is regulated through the phosphatidylinositol 3-kinase/AKT/mammalian target of rapamycin pathway. Endocrinology 2007, 148:2532–2541

Lung Cancer 70 (2010) 94–102

Contents lists available at ScienceDirect

Lung Cancer

journal homepage: www.elsevier.com/locate/lungcan

Activation status of receptor tyrosine kinase downstream pathways in primary lung adenocarcinoma with reference of *KRAS* and *EGFR* mutations

Miyako Hiramatsu[a,b], Hironori Ninomiya[a], Kentaro Inamura[a], Kimie Nomura[a], Kengo Takeuchi[a], Yukitoshi Satoh[a,d], Sakae Okumura[d], Ken Nakagawa[d], Takao Yamori[c], Masaaki Matsuura[e], Toshiaki Morikawa[b], Yuichi Ishikawa[a,*]

[a] *Division of Pathology, The Cancer Institute, Japanese Foundation for Cancer Research (JFCR), 3-8-31 Ariake, Koto-ku, Tokyo 135-8550, Japan*
[b] *Department of Thoracic Surgery, Tokyo Jikei University of Medicine, Japan*
[c] *Division of Molecular Pharmacology, The Cancer Chemotherapy Center, Japanese Foundation for Cancer Research (JFCR), Japan*
[d] *Department of Thoracic Surgical Oncology, The Cancer Institute Hospital, Japanese Foundation for Cancer Research (JFCR), Japan*
[e] *Division of Cancer Genomics, The Cancer Institute, Japanese Foundation for Cancer Research (JFCR), Japan*

ARTICLE INFO

Article history:
Received 16 September 2009
Received in revised form 2 December 2009
Accepted 5 January 2010

Keywords:
Lung adenocarcinoma
Receptor tyrosine kinases
Survival
Akt
TTF-1
Signal pathway

ABSTRACT

The activation status of signal transduction pathways involving receptor tyrosine kinases and its association with *EGFR* or *KRAS* mutations have been widely studied using cancer cell lines, although it is still uncertain in primary tumors.

To study the activation status of main components of growth factor-induced pathways, phosphorylated Akt (pAkt), extracellular signal-regulated kinases 1 and 2 (pERK) and other downstream proteins were immunohistochemically examined using surgical samples of 193 primary lung adenocarcinomas. Also, thyroid transcription factor-1 (TTF-1) expression and mutation status of *EGFR* and *KRAS* were examined.

Advanced tumor stages ($p < 0.001$), negative TTF-1 expression ($p < 0.001$) and Akt activation ($p = 0.015$) were independent and significant poor prognostic markers. Akt activation related to advanced stage ($p = 0.021$), invasiveness ($p = 0.004$), and not to mutations. TTF-1 expression associated with never-smoker ($p = 0.013$), pre- or minimally invasiveness ($p < 0.001$) and *EGFR* mutations ($p = 0.017$) as well as with pERK ($p = 0.039$) expression. *EGFR* mutations did not correlated with pAkt and pERK expression, which was different from the results based on cultured cells, while *KRAS* mutations were solely and significantly linked to ERK activation ($p = 0.009$).

In lung adenocarcinoma, tumors with TTF-1 expression have distinct characteristics regarding mutations, signal protein activation and clinical issues. Moreover, this property was revealed to be important in outcome estimation at any tumor stage, whereas Akt activation is abnormally affected according to the tumor stage regardless of their cell origin. The signal proteins were differently related to mutation status from cultured cells.

1. Introduction

Lung cancer is one of the leading causes of cancer-related deaths worldwide [1] and adenocarcinoma is recently becoming a frequent histologic type among non-small-cell lung cancers (NSCLCs) in many countries. Gefitinib, an inhibitor of epidermal growth factor receptor (*EGFR*) tyrosine kinase, has shown remarkable efficacy for control of a subset of lung adenocarcinomas, reflecting improved understanding of the underlying biology [2]. Especially the detection of somatic mutations in *EGFR* shed light on the mechanisms of acquisition of tumor growth advantage, featuring dysregulated signal transduction in tumor cells [3,4].

Akt, a serine/threonine kinase, and extracellular signal-regulated kinases 1 and 2 (ERK) are major target proteins, downstream of EGFR and various other oncoproteins such as Ras and Raf. They are known to be activated in a wide spectrum of human cancer together with various downstream substrates such as glycogen synthase kinase 3-beta (GSK3B), mammalian target of Rapamycin (mTOR), p70 ribosomal protein S6 kinase (S6K) and forkhead proteins FKHR/FKHRL1 (FKHR) [5–8] and to play central roles in tumorigenesis or cell proliferation. The present study was performed to elucidate, by immunohistochemistry (IHC), whether there might be selective activation of downstream pathways of receptor tyrosine kinases (RTKs) in lung adenocarcinomas, depending on tumor-cell lineage or with/without *EGFR* and *KRAS* mutations. We further evaluated the clinicopathological and prognostic significance of such activation in various adenocarcinoma subtypes. Since we earlier revealed by expression profiling that

* Corresponding author. Tel.: +81 3 3570 0448; fax: +81 3 3570 0558.
E-mail address: ishikawa@jfcr.or.jp (Y. Ishikawa).

0169-5002/$ – see front matter © 2010 Elsevier Ireland Ltd. All rights reserved.
doi:10.1016/j.lungcan.2010.01.001

adenocarcinoma cell lines might have different characteristics of gene expression from clinical adenocarcinomas [9], we here used tissue materials of surgically resected adenocarcinomas rather than cell lines.

2. Materials and methods

2.1. Patients and pathological review

A series of 193 Japanese cases with primary lung adenocarcinoma surgically resected between 1998 and 2001 at the Department of Thoracic Surgical Oncology, The Cancer Institute Hospital, Japanese Foundation for Cancer Research (JFCR), Tokyo, were selected for the present study. Informed consent was obtained from all the subjects at the time of surgery. This study was approved by the Institutional Review Board of the JFCR. All patients were staged pathologically according to the 5th edition of the UICC-TNM staging system [10]. For accuracy of survival analysis, only death of lung cancer was counted as cause-specific death. Smoking history was ascertained with all patients in detail.

Histological diagnosis was made according to the WHO classification [11], using sections through the largest cut surface of each tumor stained by hematoxylin–eosin and alcian-blue methods and PAS reaction. However, with its subdivision of lung adenocarcinomas, more than 80% tumors fell into the mixed subtype category. We therefore additionally used an noninvasive/invasive dichotomy as well as a predominance classification for invasive carcinomas, which is mostly based on the WHO classification except for the mixed subtype, such as bronchioloalveolar carcinoma (BAC) predominant, papillary predominant, acinar predominant, etc. The noninvasive carcinoma includes BAC. In the predominance classification of invasive carcinomas, we diagnosed by a component that makes up the predominant portion in the largest cut surface, or the cut surface containing a solid part shown by CT scans, of a tumor. Also, we employed a concept of "minimally invasive adenocarcinomas", which were defined to be lesions where an invasive area of less than 5 mm in diameter or less.

2.2. Tissue microarrays

Tumor tissues were fixed in 15% neutral formalin and embedded in paraffin. Three histologically representative sites were selected per tumor, considering the well-known heterogeneity of lung adenocarcinomas (including the peripheral boundary and the central part of each tumor) and tissue microarrays were constructed as follows. Selected points of the donor paraffin blocks of the largest cut surface were punched with a 2-mm-diameter coring needle, and transferred to the array in the recipient block using a manual tissue arrayer (KIN-1, Azumaya, Inc, Japan). 48 human tissue rods (16 tumors) were embedded in one tissue array block. Based on our preliminary examinations using whole sections of tumor for several cases, we adopted 2 mm needles and three points to take tissues, rather than smaller needles and only one or two points. As controls, 3 mouse xenografts were selected from the panel of 39 cell lines (termed JFCR 39) [12] and embedded together with clinical samples in each array block as detailed below.

2.3. Protein expression analysis

Phosphorylated protein levels of Akt, ERK, GSK3B, mTOR, S6K and FKHR were immunohistochemically examined using antibodies for phosphorylated proteins designated by pAkt, etc. Also, thyroid transcription factor-1 (TTF-1) was examined for cell lineage analysis. The primary antibodies and citrate buffer used in this study are listed in Suppl. Table 1 and details of our immunohistochemical technique are also available on this. Antigen–antibody complexes were detected by labeling with the Envision+/HRP system (DAKO, Carpinteria, CA, USA), using 3,3′-diaminobenzidine tetrachloride as the chromogen and hematoxylin as counterstain. As well as using some normal cells as internal controls, mouse xenografts of the three cancer cell lines (PC-3, a prostate cancer line, showing high pAkt and low pERK expression, U251, a brain tumor line, showing moderate pAkt and low pERK expression and HTB26, a breast cancer line, showing low pAkt and high pERK expression) were included as external controls (Fig. 1), because we sought better quantification of immunoreactivity of each antibody by using well-known cell lines with well-documented reactivity. Immunoreactivity of each case was evaluated for all the tumor cells (or other cells of interest) appearing in all the three portions, applying the staining results for these xenografts. Essentially, for pAkt and pFKHR cytoplasmic staining (Fig. 1 and Suppl. Fig. 1), and for pS6K and pGSK3B whole cell staining were evaluated respectively, referring to the U251 levels. For pmTOR staining, comparison was with HTB26. All these were recorded as dichotomous parameters categorized as "negative" (weaker than or equal to xenograft staining) and "positive" (stronger than xenograft staining). For pERK immunoreactivity, the percentages of cells with positive staining were recorded and a score of 10% or less was categorized as "negative" and a score of more than 10% as "positive".

2.4. Mutation analysis of EGFR and KRAS

The mutation status of four exons of the *EGFR* gene and three codons of the *KRAS* gene was evaluated in the subset ($n = 93$) of the 193 cases. The primer sequences for exons 18 and 21 of *EGFR* were as follows (forward and reverse, respectively), exon 18 (5′-TCCAAATGAGCTGGCAAGTG-3′ and 5′-TCCCAAATACTCAGTGAACAAA-3′), exon 21 (5′-GATGCAGAG-CTTCTTCCCAT-3′ and 5′-ATACAGCTAGTGGGAAG GCA-3′). For *KRAS*, codon 12 and codon 13 (5′-CCTTATGTGTGACATGTTCT-3′ and 5′-CTATTGTTGGATCATATTCG-3′), codon 61 (5′-TTCC-TACAGGAAGCAAGTA-3′ and 5′-GGCAAATACACAAAGAAAGC C-3′). All PCR assays were carried out in a 20 μL volume that contained 0.2 μL of Taq DNA polymerase (NEB Phusion TM High Fidelity DNA polymerase sets, Finnzymes Oy, Finland). DNA was amplified for 35 cycles at 98 °C for 10 s, 60 °C for 30 s, and 72 °C for 30 s, followed by a 7 min extension at 72 °C. All PCR products were incubated with exonuclease I and shrimp alkaline phosphatase (USB corporation, Exo SAP-IT, OH, USA) according to the manufacturer's instructions and then sequenced directly by a cycle sequencing method (Beckman Coulter Inc, DTLS-Quick Start Kit, CA, USA). All sequence variants were confirmed by sequencing the products of independent PCR amplifications in both directions. To detect deletion in exon 19 and insertion in exon 20 of *EGFR*, common fragment analysis was used. Sample DNA was amplified with a Cy5-labeled primer set as follows: exon 19 (5′ Cy5-GTCTTCCTTCTCTCTCTGTCAT-3′ and 5′-TGTGGAGA GTGAGCAGGGTCT-3′), exon 20 (5′ Cy5-A CCATGCGAAGCCACACTGA-3′ and 5′-TCCTTATCTCCCCTCCCCGTAT-3′) and any deletion or insertion mutation was detected as a new peak of amplified products in the electrophoregram.

2.5. Statistical analysis

Statistical analyses were accomplished with STATA software, version 9 (Stata Corp. LP, College Station, TX, USA) and statistical programming language of R [13]. We studied the relationships between the survival and other clinicopathological factors and phospho-protein expression by univariate analyses of log-rank test. Then multivariate analyses using Cox regression model together with an AIC (Akaike Information Criteria) stepwise selection were applied to those factors to evaluate their relative risks. Then, correlation coefficients between each clinicopathological or

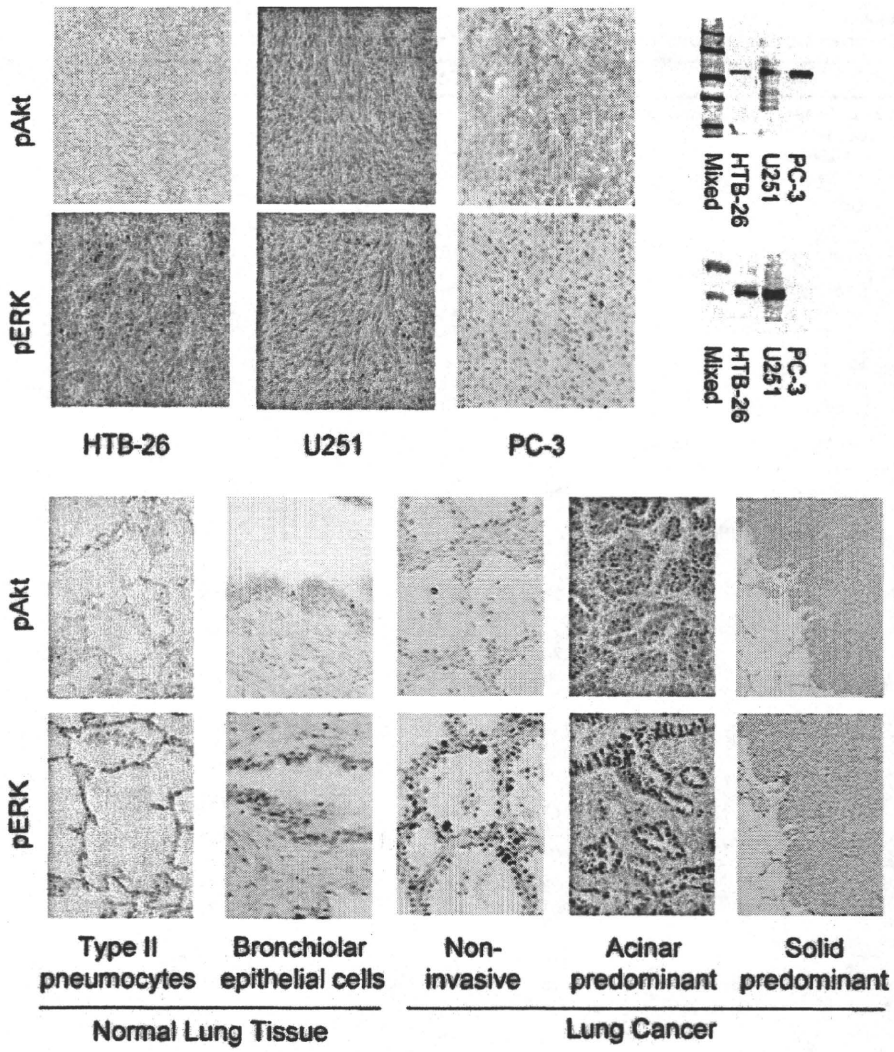

Fig. 1. Immunohistochemical staining of xenografts with specific antibody against pAkt (the upper row) and pERK1/2 (the lower row). (a) HTB-26; xenograft of breast cancer cell negative for pAkt and positive for pERK1/2; (b) U251; xenograft of glioma cell moderately positive for both pAkt and pERK1/2; (c) PC-3; xenograft of prostate cancer cell positive for pAkt and negative for pERK1/2. Almost all the cells with mitotic figure were scattered and were positive for pERK1/2. Immunohistochemical staining of resected lung specimen with specific antibody against pAkt (the upper row) and pERK1/2 (the lower row). Normal lung tissues (left side) and lung adenocarcinoma of noninvasive, acinar predominant and solid predominant histology (the right side). See that pAkt is almost homogeneously stained compared to that of pERK1/2.

immunohistochemical parameter were calculated and *p*-values for the statistical significance were given by a two-tails test checking a null hypothesis about zero Pearson's correlation coefficient between two variables.

Two-sided *p*-value below 0.05 was designated statistically significant.

3. Results

Patient characteristics of the 193 cases and differences in survival according to each clinicopathological factor or protein expression were shown in Table 1.

3.1. Patients and pathological review

The gender distribution was equal, the median age was 63 years and the median follow-up period was 2066 days (5.66 years) (ranged 133–3292 days). Pathological review revealed that more than 80% of the cases were classified as the adenocarcinoma with mixed subtype according to the current WHO classification. Therefore results based on the predominance classification together with invasive/noninvasive dichotomy were presented here. 22.8% ($n=44$) of the cases were classified as pre- and minimally invasive adenocarcinomas. The rest (77.2%; $n=149$) were invasive adenocarcinoma in which papillary (including micropapillary), acinar, solid patterns or patterns of other variants are predominantly recognized. The rates were 61.1% ($n=118$), 9.9% ($n=19$) and 6.2% ($n=12$), respectively.

3.2. Immunohistochemical study and the EGFR/KRAS mutation status

We observed rather homogeneous and tumor-specific staining patterns for pAkt although the intensity was low, 37.8% (73/193) of surgically excised lung adenocarcinomas being positive. The positive rates for pGSK3B, pmTOR, pS6K, pFKHR and TTF-1 were 30.6% ($n=59$), 34.7% ($n=68$), 52.3% ($n=101$), 40.4% ($n=78$) and 79.8% ($n=154$), respectively. The pERK staining pattern was characteristically heterogeneous. The rate of positive tumor cells ranging from 5% to 100% and the staining was not tumor-cell specific but rather